Ph.D DISSERTATION

A STUDY ON PRACTICAL ISSUES FOR IMPLEMENTATION OF WIRELESS POWER TRANSFER SYSTEM

무선전력전송시스템을 구현하기 위한 실질적인 문제에 관한 연구

BY
JONGMIN PARK

AUGUST 2014

SCHOOL OF ELECTRICAL ENGINEERING AND
COMPUTER SCIENCE COLLEGE OF ENEGINEEING
SEOUL NATIONAL UNIVERSITY

공학박사 학위논문

A STUDY ON PRACTICAL ISSUES FOR IMPLEMENTATION OF WIRELESS POWER TRANSFER SYSTEM

무선전력전송시스템을 구현하기 위한 실질적인 문제에 관한 연구

2014년 8월

서울대학교 대학원

전기·컴퓨터 공학부

박 종 민

Abstract

This thesis presents solutions of the practical issues for implementation of wireless power transfer system (WPTS). There are many unresolved issues that remain in the implementation of highly efficient WPTS. To solve the adaptive matching and multiple charging problems, new methods are proposed. Also, to analyze the effect of surroundings of a WPTS, characteristic mode method was suggested.

First, adaptive matching methods for a WPTS in the near-field region are investigated. The impedance and resonant frequency characteristic of a near-field power transfer system are analyzed according to coupling distance. In the near-field region, adaptive matching is necessary to achieve an effective power transfer. We compare the power transfer efficiencies of several schemes including simultaneous conjugate matching and frequency tracking. It is found that effective adaptive matching can be easily achieved by tracking the split resonant frequency. In addition, a modified frequency tracking method is proposed to extend the range over which the power is transmitted with high efficiency. The experimental results are in agreement with the theoretical results.

Secondly, we found the optimal conditions for an efficient WPTS. Additionally, we found that a class-D PA has an advantage as a source when the input resistance

changes with the position of the receiving antenna. The proposed WPTS was verified through the experimental results.

Thirdly, a multiple charging method for a wireless power transfer system in the near-field region is proposed. We analyzed the frequency characteristics of multiple receivers in the near-field region. The results suggested that the time division WPTS can achieve efficient and equal power transmission at multiple receivers. We conclude that this system has an advantage for charging multiple receivers.

Finally, the effect of the surroundings for a WPTS was investigated. The characteristic mode method was suggested to analyze the effect of the surroundings. For electrically small and intermediate size bodies, only a few characteristic modes are needed to characterize the electromagnetic behavior of the body. The theory is verified by a simulation with small loops and a metal plate.

Keywords: near-field coupling, wireless power transfer (WPT), adaptive matching, frequency tracking, resonant coupling, class-D PA, control of load resistance, multiple charging, time sharing, characteristic mode.

Student number: 2008-30876

Contents

List of Figures

List of Tables

Chapter 1

Introduction

Wireless power transfer (WPT) is has long been a topic of interest. In 1891, Nikola Tesla demonstrated wireless energy transmission by means of electrostatic induction using high tension induction coil [1]. But Tesla coils involved undesirably large electric fields. Recently, WPT using near-field coupling receive attention again [2]-[11]. The authors of [2] used the coupled mode theory to analyze the characteristics of near-field WPT. They demonstrated efficient power transfer between two coupled helical type antennas at the resonant frequency as shown in Fig. 1.1. The measured efficiency was about 40% at a distance of 2 m. They also demonstrated that the efficiency could be improved by putting a mediating resonant antenna between the transmitting and receiving antennas [6].

Fig. 1.1 MIT WPTS prototype

Also, the frequency characteristic of near-field coupled antennas that are used for WPT has been studied using the same theory [7]. An alternative analysis method was presented using spherical modes and an addition theorem [8]. The frequency characteristic was also derived using this method [9]. The analysis method using spherical modes gives a clear physical limitation of wireless power transfer system (WPTS) using near field coupling. The theoretical basis basic study has been progressed briskly. However, there are many unresolved issues that remain in the implementation of highly efficient WPTS.

Fig. 1.2 WPTS indoors

In this dissertation, a study on practical issues for implementation of a WPTS. Firstly, it is known that the optimum source and load impedance vary drastically with the coupling distance and the orientation of the antennas [8]. So, it is important to realize an adaptive matching system for efficient power transfer in the near-field region. Secondly, a study on multiple device charging issue is done. Thirdly, the effect of the surroundings of the WPTS is investigated.

1.1 WPT Scenario

Fig. 1.2 shows a WPT scenario indoors. Transmitting device is located at ceiling and various receiving devices are indoors. There are many issues to realize WPTS in this situation. Firstly, the position of receiving devices are varied. So the coupling between transmitting and receiving devices are varied. Therefore adaptive matching is demanded for efficient WPT. Secondly, the method for multiple charging is needed to charge multiple receiving devices at the same time. Fig. 1.3 shows the multiple charging case of electrical devices. Coupling between transmitter and receivers are dependent each other. So it is hard to control the behavior of the system. The solution is needed for multiple charging.

Fig. 1.3 Multiple electric devices charging

Fig. 1.4 Receiver of WPTS

Finally, the surroundings of the WPTS is considered. Fig. 1.4 shows receivers for WPT. The spiral antenna is located on the electrical device. The device can have a great effect on WPTS. So the effect of surroundings are considered when WPTS is implemented.

1.2 Characteristics of WPT

The authors of [8] used spherical modes and an addition theorem to analyze the characteristics of near-field WPT. Generally, the WPTS operates at a very low frequency, with the result that the size of the antennas in the system is very small. Therefore, we can assume that an antenna in a WPTS is a quasi-canonical minimum scattering (CMS) antenna.

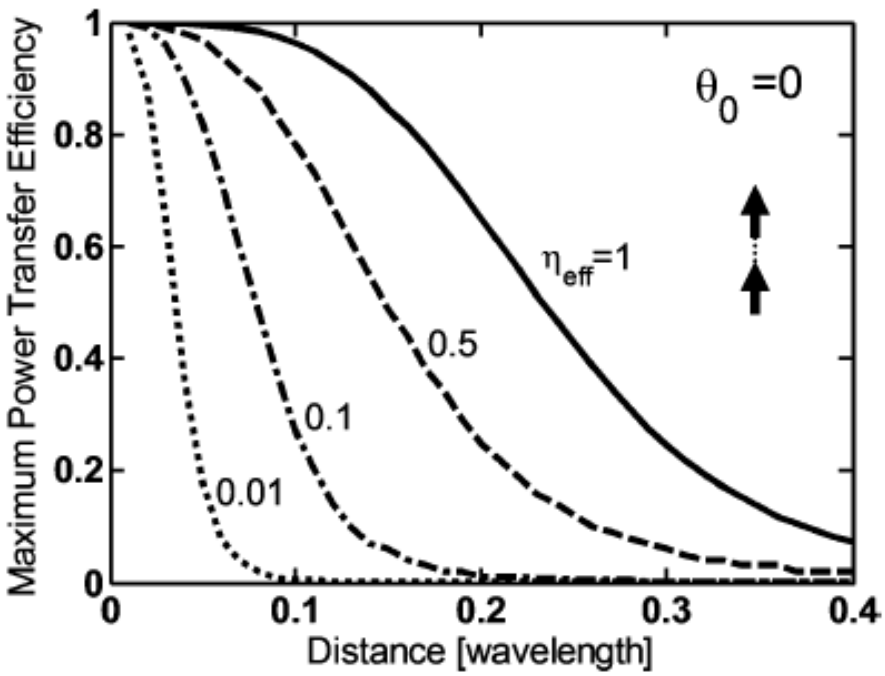

Fig. 1.5 The maximum power transfer efficiencies of antennas with different radiation efficiencies [8]

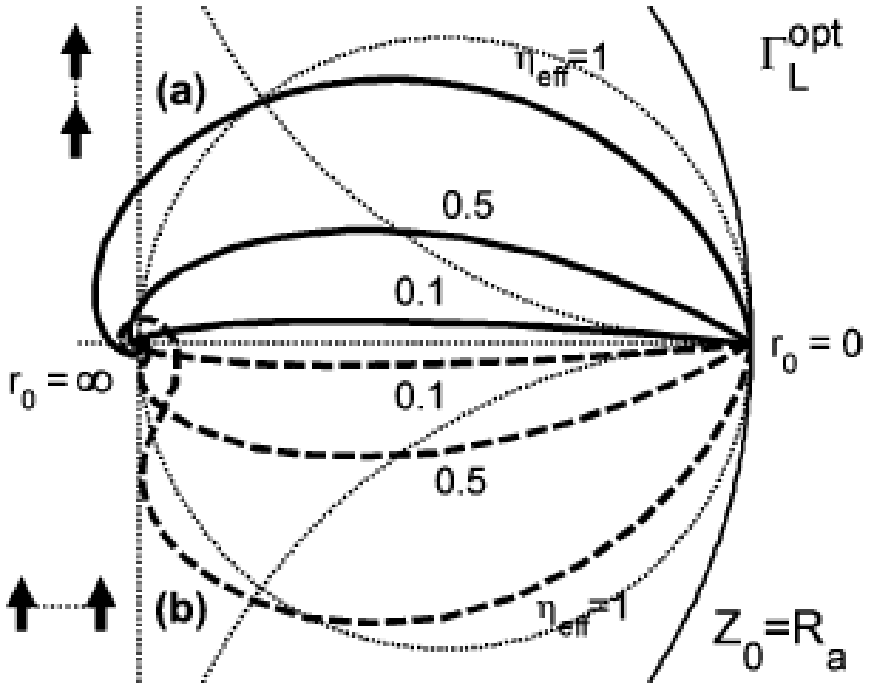

Fig. 1.6 The Smith chart representation of the optimum load impedances of antennas with different radiation efficiencies [8]

A CMS antenna is defined as one that becomes invisible when the antenna port is open-circuited [12]. Also, a small antenna generates only one fundamental spherical mode. To derive the Z-parameter between two antennas, The authors of [8] express antennas as the generalized scattering matrix. Z-parameter of two coupled antennas

can be obtained by solving the generalized scattering matrix. Optimum load impedance and maximum power transfer efficiency when two identical CMS antennas are coupled were given in [8]. From (8), the higher the radiation efficiency of an antenna is, the higher the maximum power transfer efficiency is. The maximum power transfer efficiency of a WPTS for several radiation efficiencies is shown in Fig. 1.5. The maximum power transfer efficiency only depends on the radiation efficiency of antennas and distance between antennas. Also, the optimum load impedance for varying distance between antennas is shown in Fig. 1.6. The optimum source and load impedance vary drastically with the coupling distance and the orientation of the antennas. So adaptive matching is very importance issue to implement highly efficient WPTS.

Reference

[1] "Experiments With Alternating Currents of Very High Frequency, and Their Application to Methods of Artificial Illumination," Columbia College, 1891.

[2] M. Soljacic, “Wireless energy transfer can potentially recharge laptops, cell phones without cords,” Report in San Francisco Massachusetts Institute of Technology, 2006.

[3] A. Kurs, A. Karalis, R. Moffatt, J. D. Joannopoulos, P. Fisher, and M. Soljacic, “Wireless power transfer via strongly coupled magnetic resonances,” *Sciencexpress*, Jun. 7, 2007.

[4] M. Soljacic, E. H. Rafif, and A. Karalis. “Coupled-mode theory for general free-space resonant scattering of waves” *Physical Review*, vol. 75, no.5, pp.1-5, 2007.

[5] A. Karalis, J. D. Joannopoulos, and M. Soljacic, “Efficient wireless non-radiative mid-range energy transfer,” *Annals of Phys*ics, vol. 323, pp.34-48, Jan. 2008.

[6] R. E. Hamam, A. Karalis, J.D. Joannopoulos, and M. Soljacic, “Efficient weakly-radiative wireless energy transfer: An EIT-like approach,” *Annals of Physics*, vol. 324, pp. 1783-1795, Aug. 2009.

[7] Y. Kim and H. Ling, "Investigation of coupled mode behaviour of electrically small meander antennas," *Electron. Lett.*, vol.43, no.23, Nov. 2007.

[8] J. Lee and S. Nam, “Fundamental aspects of near-field coupling antennas for wireless power transfer,” *IEEE Trans. Antennas and Propag*., submitted for publication.

[9] Y. Tak, J. Park, and S. Nam, "Mode-Based Analysis of Resonant Characteristics for Near-Field Coupled Small Antennas," *IEEE Antennas and Wireless Propag. Lett.,* vol. 8, pp. 1238-1241, Nov. 2009.

[10] T.S. Bird, et al., "Antenna impedance matching for maximum power transfer in wireless sensor networks", *IEEE SENSORS 2009*, October 2009, Christchurch, New Zealand, pp. 916-919 .

[11] W. Fu, B. Zhang, and D. Qiu, “Study on frequency-tracking wireless power transfer system by resonant coupling,” *Power Electronics and Motion Control Conf., 2009. IPEMC '09. IEEE 6th International 2009*, pp. 2658 – 2663.

[12] W. K. Kahn and H. Kurss, “Minimum-Scattering Antennas,” *IEEE Trans. Antennas and Propag.*, vol. 13, no. 5, pp. 671-675, Sep. 1965.

Chapter 2

Investigation of Adaptive Matching Methods for Near-Field WPT

2.1 Introduction

WPT has long been a topic of interest. Research on WPT using near-field coupling has recently been reported [1]-[10]. The authors of [1] used the coupled mode theory to analyze the characteristics of near-field WPT. They demonstrated efficient power transfer between two coupled antennas at the resonant frequency. The measured efficiency was about 40% at a distance of 2 m. They also demonstrated that the efficiency could be improved by putting a mediating resonant antenna between the transmitting and receiving antennas [5]. The frequency characteristic of near-field coupled antennas that are used for WPT has been studied using the coupled mode theory [6]. The authors of the paper explain the resonant frequency splitting phenomenon in strongly coupled regions and study the characteristics of input impedance and power transfer efficiency at split modal resonant frequencies.

An alternative analysis method was presented using spherical modes and an

addition theorem [7]. This method showed that maximum power transfer efficiency and optimum load impedance can be obtained using the characteristics of a single antenna. The frequency characteristic was also derived using mode-based analysis [8].

A WPTS requires high efficiency power transmissions anywhere in the near-field range. However, there are many unresolved issues that remain in the implementation of highly efficient WPTS. First of all, it is known that the optimum source and load impedance vary drastically with the coupling distance and the orientation of the antennas [7]. Hence, it is important to realize an adaptive matching system for efficient power transfer in the near-field region. To improve power transfer efficiency in cases of varying distance between two antennas, some methods were suggested [9], [10]. One method achieved an adaptive matching by tuning the antenna and matching network [9]. But this method is difficult to accomplish practically. The frequency tracking method was suggested in [10] using a model of a resonant coupling circuit. However, in that study, the limitation of the method and the effect of the load impedance were not shown. In this paper, we study the characteristics of several adaptive matching methods, such as conventional simultaneous conjugate matching and frequency tracking. During the investigation, we discovered the limitation of the frequency tracking method and proposed a modified frequency tracking method that makes efficient power transfer possible

without simultaneous conjugate matching. The modified frequency tracking method is demonstrated using center-fed spiral antennas with a self-resonant frequency of 10.02 MHz. Potential applications of this idea include WPTS, domotics, WBAN (Wireless Body Area Network), OLEV (On-Line Electric Vehicle), and NFC (Near Field Communication).

2.2 Impedance Characteristic of Coupled Antennas

Power can be transferred efficiently when two antennas are located in close proximity to one another. This near-field coupling phenomenon between antennas can be explained effectively by the coupled mode theory [2], [11]. From [2], the optimum load resistance for maximum power transfer efficiency is represented as:

$$R_L^{opt} = R_R \sqrt{1 + k^2 \frac{4L_T L_R}{R_T R_R}} \tag{2.1}$$

where the subscripts T, R, and L mean the transmitter, the receiver, and the load, respectively. R_T and R_R, which are the respective resistances of the transmitter and the receiver, are composed of the radiation and ohmic resistance of the antenna. L_T and L_R are the inductance at the transmitter and the receiver, respectively. k is the coupling coefficient between the antennas. The coupling coefficient varies according to the distance between the antennas. Because the optimum load impedance is a function of the coupling coefficient, it also varies based on the distance between the antennas. Therefore, it is necessary to simultaneously satisfy the matching condition at both the transmitting and receiving ports in order to achieve maximum power transfer efficiency. However, simultaneous matching is difficult to implement.

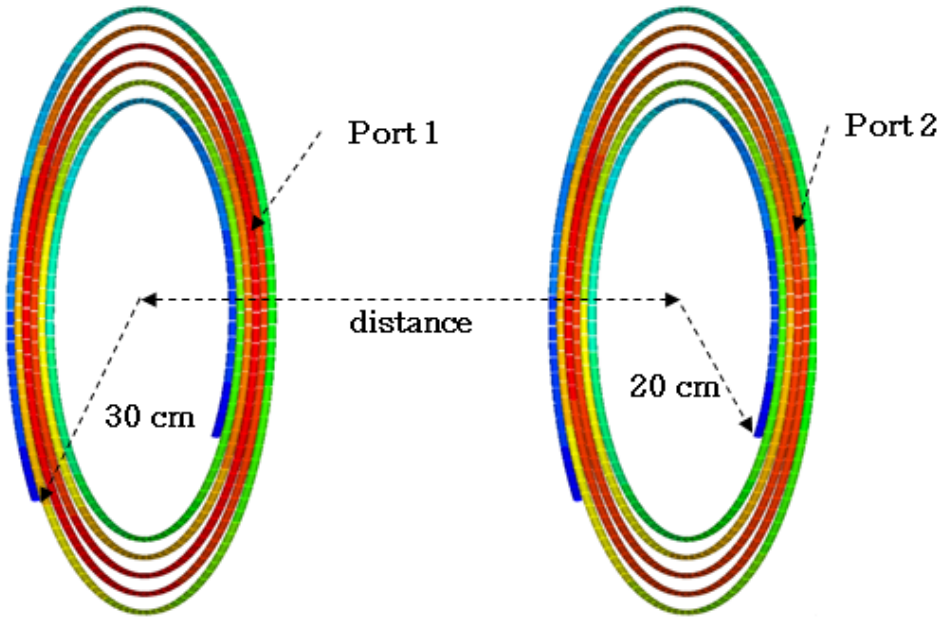

Fig. 2.1 Center-fed spiral antenna (outer radius = 30 cm, inner radius = 20 cm, wire thickness = 5 mm, 5.7-turns, self-resonant frequency = 10.02 MHz).

As an example, we consider center-fed 5.7-turn electrically small spiral antennas made of copper wire, as shown in Fig. 2.1. The outer and inner radii are 30 and 20 cm, respectively. The wire diameter is 5 mm and the self-resonant frequency of the antenna is approximately 10.02 MHz. The receiving and transmitting antennas are identical. In this case, magnetic coupling is dominant, so that the formula for the coupling coefficient is given as $k=\omega M / [2(\Gamma_T\Gamma_R)]1/2$, where M is the mutual inductance between the two antennas. The intrinsic decay rate is $\Gamma_m = R_m / 2L_m$, where R_m and L_m are the resistance and the inductance of antenna m, respectively.

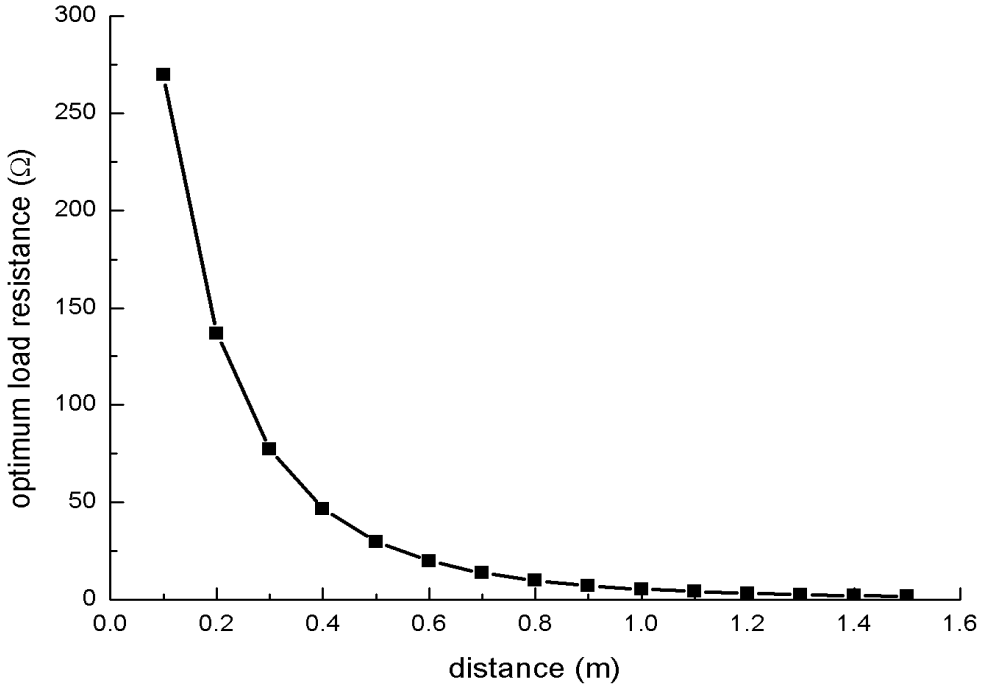

Fig. 2.2 The optimum load resistances versus the distance between the antennas.

Then, the optimum load resistance is represented as:

$$R_L^{opt} = (R_o + R_r)\sqrt{1 + \frac{(\omega M)^2}{(R_o + R_r)^2}} \tag{2}$$

where R_o and R_r are the ohmic resistance and the radiation resistance of the antenna, respectively. The mutual inductance was obtained using the electromagnetic theory [2], and the resistances of the single antennas were obtained using an EM simulation. The simulation was performed using FEKO, a commercially available software that

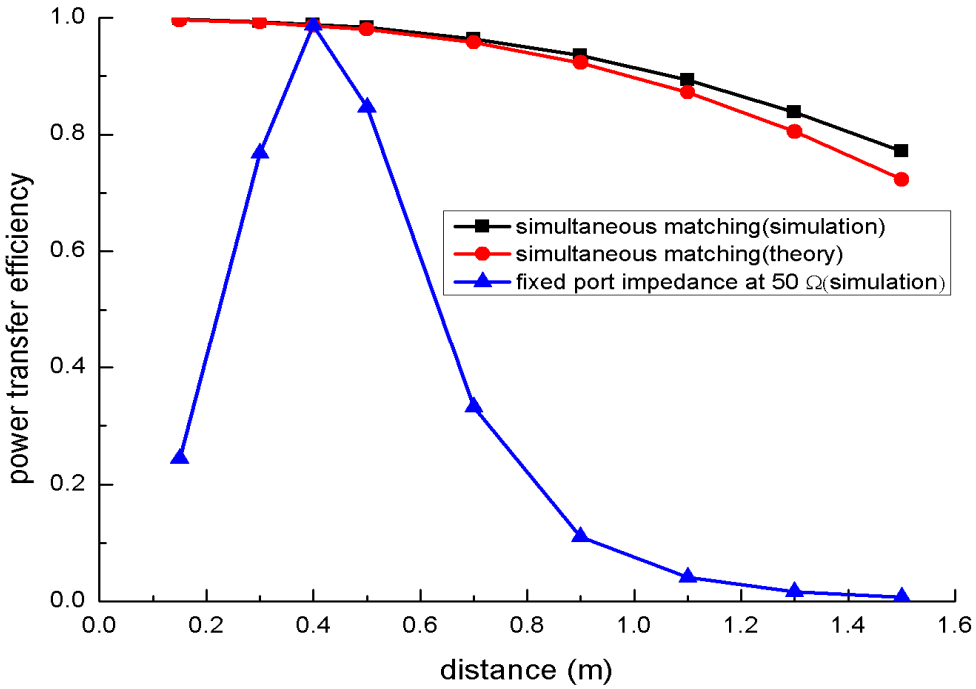

Fig. 2.3 The optimum load resistances versus the distance between the antennas.

is based on the Method of Moments (MOM) technique. Figure 2.2 shows the optimum load impedance versus the distance between the two spiral antennas. When the two antennas get closer, the optimum resistance for the maximum power transfer varies quite drastically. Therefore, it is very difficult to realize an adaptive simultaneous matching circuit on both the transmitting and receiving antennas. Figure 2.3 shows the maximum power transfer efficiency obtained using the coupled mode theory, EM simulation, and the power transfer efficiency with a fixed source and a load impedance of 50 ohm. The simulation results agreed with the power

transfer efficiencies from the coupled mode theory. The power transfer efficiency with a fixed port impedance of 50 ohm is inefficient almost everywhere, except at the approximate distance of 0.4 m. This is explained by the fact that the optimum load impedance is almost 50 ohms only at a distance close to 0.4 m and that the optimum load impedance sharply changes when the distance recedes from 0.4 m, as shown in Fig. 2.2.

2.3 Frequency Characteristic of Coupled Antennas

When two resonant antennas are strongly coupled with each other in a near-field region, the resonant frequency is split [6], [10]. The split resonant frequencies are determined by the amount of coupling between the antennas. Input impedances at the split resonant frequencies for coupled small antennas have recently been investigated [6]. We noticed that the input impedance at the split resonant frequency is almost equal to the load impedance in the strongly coupled region, provided that the load impedance is much greater than the ohmic resistance and the radiation resistance, as in practical systems. Therefore, it is conceived that input matching and efficient power transfer can be achieved with fixed port impedances by adjusting the frequency of the source to a desired split resonant frequency. For the spiral antennas shown in Fig. 2.1, the split resonant frequencies of the coupled antennas were obtained by a simulation using FEKO, a commercially available software. Figure 2.4 shows the simulation results of the power transfer efficiencies for the conventional simultaneous conjugate matching method and the frequency tracking method. The power transfer efficiency is calculated from the S-parameter as |S21|2. The simultaneous matching result is obtained on the condition that the frequency is fixed at the self-resonant frequency of the single antenna and that simultaneous conjugate matching is achieved whenever the distance between the antennas is varied. Maximum power transfer efficiency can be achieved using simultaneous matching.

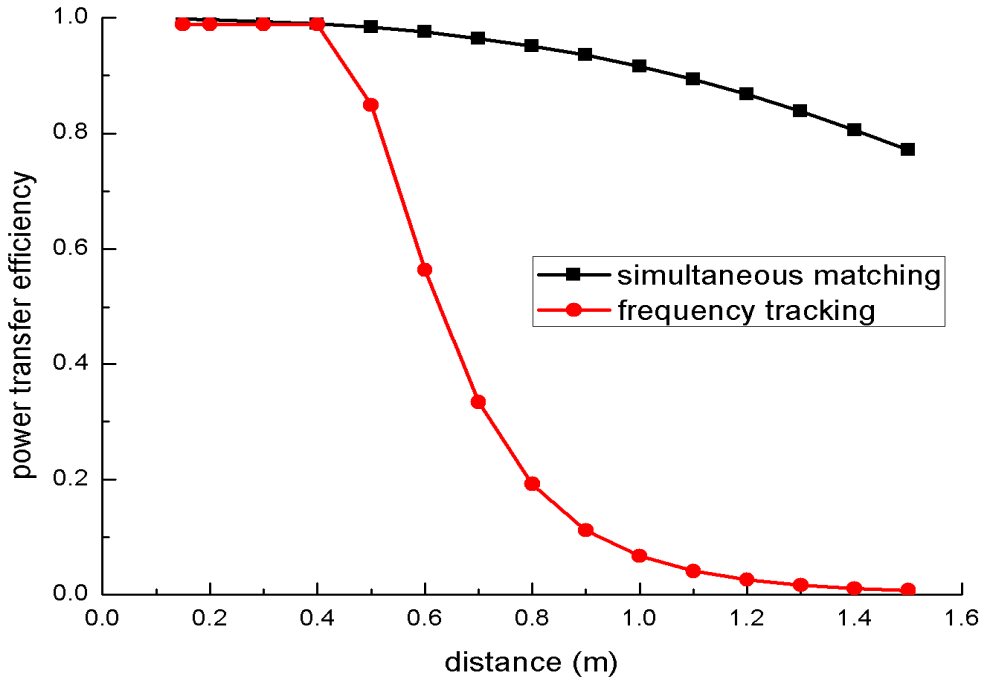

Fig. 2.4 Comparison of the power transfer efficiency of two coupled small spiral antennas.

On the other hand, the result of the frequency tracking method is based on the assumption that the system can trace the odd mode resonant frequency. The frequency tracking method can achieve almost the same efficiency as the simultaneous matching case in the strongly coupled region. Compared to adaptive simultaneous matching, it is easy to achieve input matching with the frequency tracking method, because only the source at the transmitting antenna needs to be

controlled. However, the shortcoming of the frequency tracking method is the drastic decrease of power transfer efficiency outside of the strongly coupled region. When the port impedance of the antenna is 50 ohms, the frequency tracking method is useful only in the strongly coupled region.

2.4 The Effect of Port Impedance

If it is necessary to stably transmit power outside of a strongly coupled region, then a frequency tracking method with a 50 ohm port impedance is not suitable for the system. Therefore, a modified frequency tracking method that could achieve stable power transfer over an extended range was investigated. For this purpose, the port impedances are not set to 50 ohms, but to the optimum impedance at the target distance. Then adaptive matching is performed using the frequency tracking method.

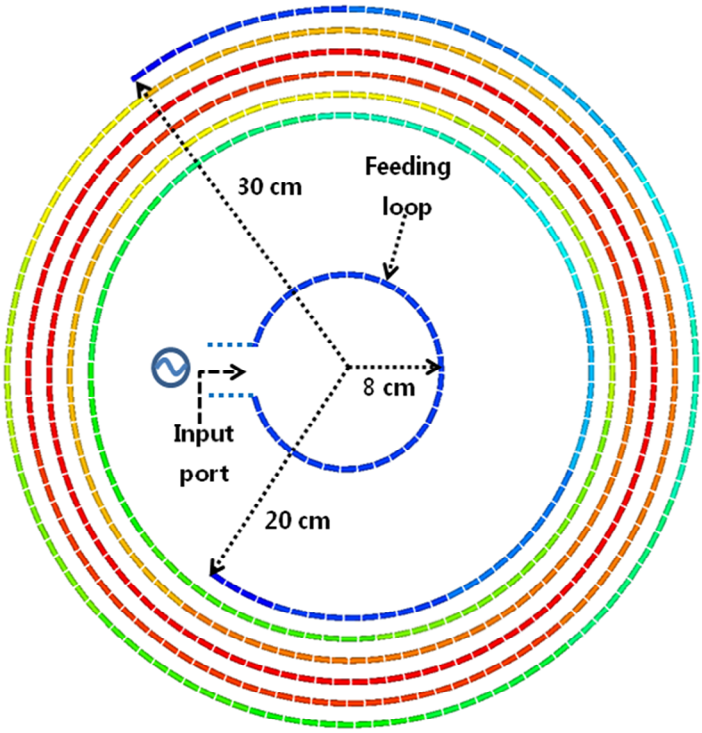

Fig. 2.5 Inductively coupled fed spiral antenna.

In the demonstration system shown in Fig. 2.5, inductive coupling is chosen to feed the antenna instead of a direct feed since it is an easy way to realize the matching circuit. The port of 50 ohms is directly connected at the feeding loop. The port impedance at the feeding loop can be converted into the optimum impedance of the spiral antenna by adjusting the inductive coupling between the feeding loop and the spiral antenna. The amount of coupling can be controlled by the size and position of the feeding loop. The optimum impedance is 2.25+j1.23 ohms at the target distance of 1.5m. To optimize the port impedance at the target distance, the loop and the spiral antenna are in the same plane and have the same axis. The radius of the loop is 8 cm.

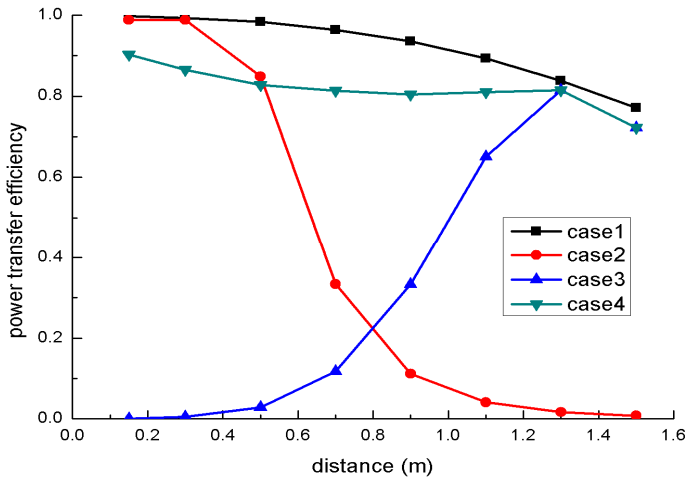

(a)

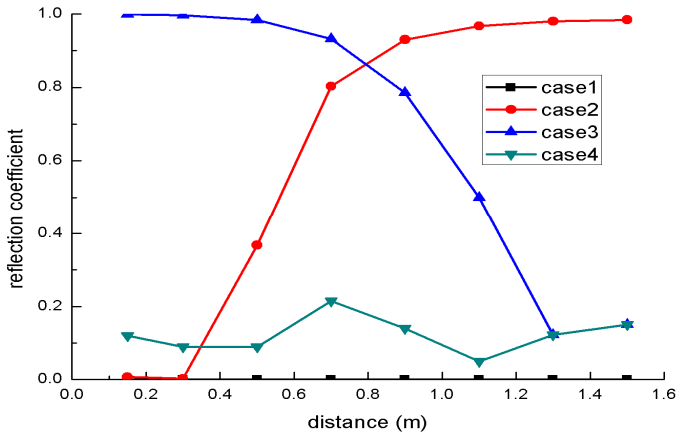

(b)

Fig. 2.6 Comparison of the return loss and the power transfer efficiency for two coupled small spiral antennas: (a) power transfer efficiency, (b) reflection coefficient at the input port (case 1: fixed frequency with simultaneous matching condition; case 2: frequency tracking with 50 ohm load impedance; case 3: fixed frequency with fixed load impedance (optimum impedance at 1.5 m); case 4: frequency tracking with fixed load impedance (optimum impedance at 1.5 m)).

Figure 2.6 shows the simulation results of the power transfer efficiency and the return loss of several adaptive matching methods. In case 1, the frequency is fixed with the simultaneous matching condition. In case 2, the frequency tracking method is used with a 50 ohm load impedance. In case 3, the frequency is fixed with the optimum load impedance at 1.5 m. Case 4 uses the modified frequency tracking method with optimum load impedance at 1.5 m. As shown in Fig. 2.6(a), case 1 performs very well but it is too difficult to realize the simultaneous matching condition for the variation of distance. The system in case 2 is efficient only in the strongly coupled region. The power transfer efficiency outside the strongly coupled region drastically decreased. Case 3 also only performs well close to the 1.5 m target distance. Case 4, the modified frequency tracking method, shows good performance up to the target distance of 1.5 m. Figure 2.6(b) shows the reflection coefficient at the input port. The impedance mismatching at the input port is the primary cause for the decrease in power transfer efficiency. Impedance matching can be achieved by the modified frequency tracking method anywhere within the 1.5 m target distance. In the strongly coupled region, the efficiency of case 4 is smaller than that of case 1 and case 2 because of the reactance of the optimum load impedance. It causes a slight impedance mismatch. Even though the power transfer efficiency is not optimal at very close distances, this method is useful to achieve stable high power transfer efficiency in the target region.

2.5 Measurements

Figure 2.7 shows photographs of the experimental setup for the demonstration of the proposed modified frequency tracking method. The structure of the antennas and feeds are the same as in the simulation model. A plastic structure is used to fix the antenna. An LED is used to check the power transmission phenomena. Figures 2.7(a) and (b) show that the system successfully works using the modified frequency tracking method at 15 cm and 150 cm, respectively. The LED, which is located at the lower right of the receiving antenna, was activated by the transferred power.

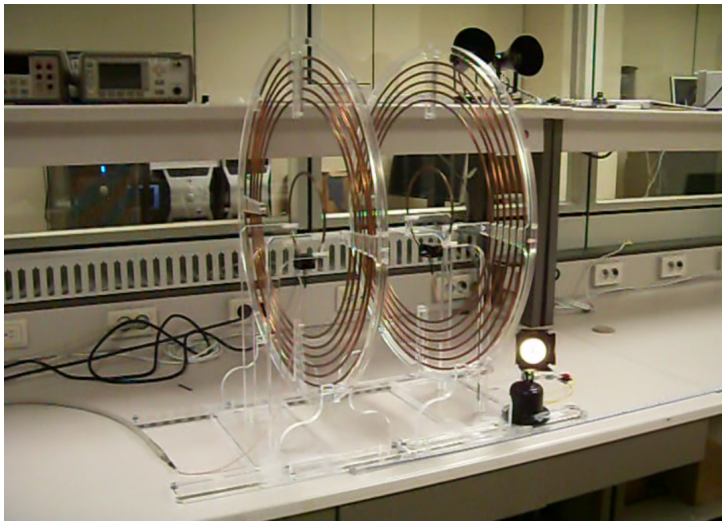

(a)

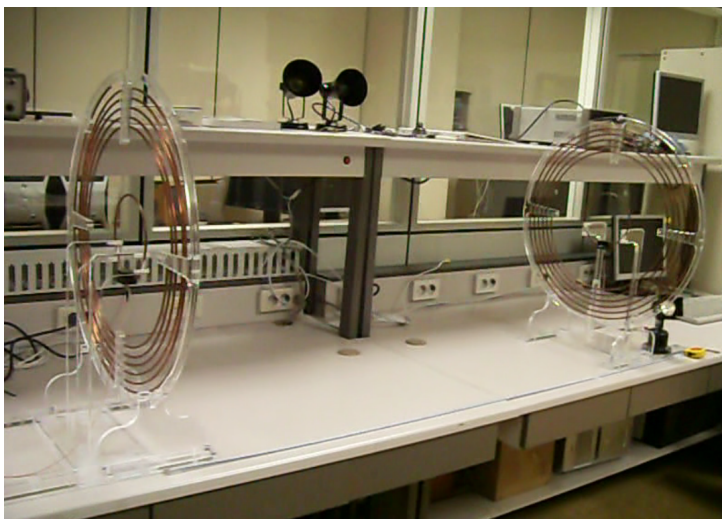

(b)

Fig. 2.7 Photograph of the WPTS using the frequency tracking method: (a) d = 15 cm, (b) d = 150 cm.

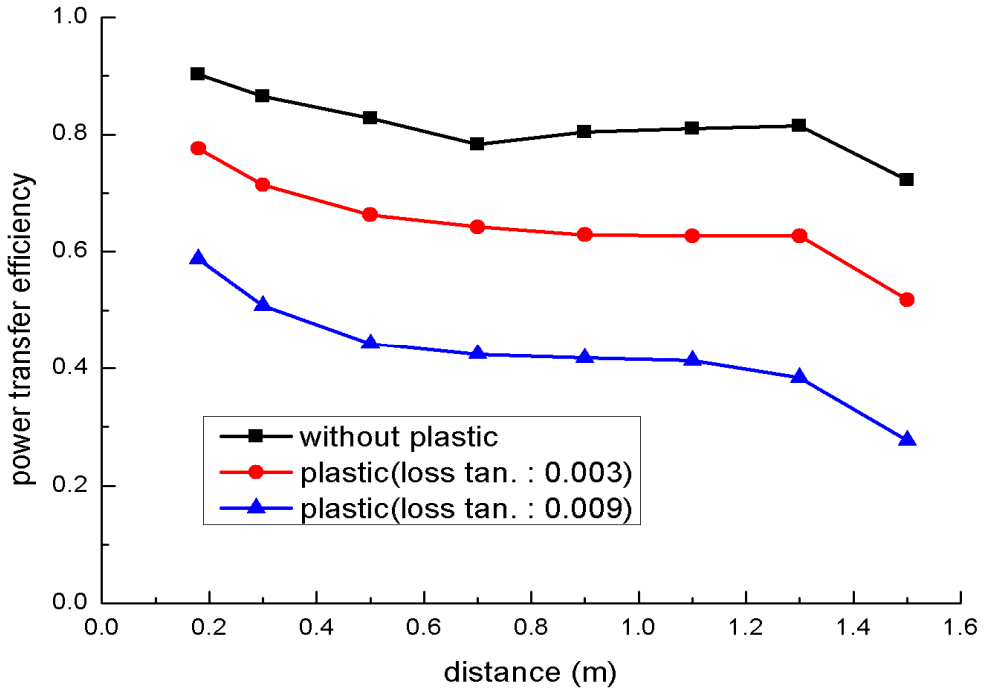

Fig. 2.8 Effect of the plastic structure on the power transfer efficiency for case 4 (dielectric constant: 3.5).

In order to fix the antenna, the dielectric loss of the plastic structure should be considered in order to estimate the transfer efficiency correctly. Figure 2.8 shows the power transfer efficiency incorporating the dielectric loss. The permittivity of the general plastic is found to vary from 2.5 to 5, and the loss tangent ranges from 0.0001 to 0.035 [12]. In our case, the dielectric constant of the plastic structure is 3.5,

and the power transfer efficiency was simulated with various loss tangents. When the loss tangent of the plastic structure increased, the power transfer efficiency decreased. When the loss tangent of the plastic was 0.009, the power transfer efficiency decreased by 30%. To precisely predict the power transfer efficiency, the plastic structure's dielectric loss should be considered. In addition, a dielectric with a low dielectric loss should be used to fix the antenna. Figure 2.9 is a comparison of the measurements and the simulation results. Figure 2.9(a) shows the resonant frequency versus the distance. The measured self resonant frequency of the antenna is approximately 9.63 MHz, which is about 4 % lower than the simulation result. This seems to be due to the dielectric structure, which causes the resonant frequency to be lower, and to manufacturing error. When the two antennas become closer, the resonant frequency changes into two split resonance frequencies at 1.3 m. The measured results agreed with the simulation results. Figure 2.9(b) shows the results of the measured and the simulated power transfer efficiency for case 4. The simulation included a dielectric structure with a dielectric constant and loss tangent of 3.5 and 0.009, respectively. The measured power transfer efficiency agreed with the simulation results.

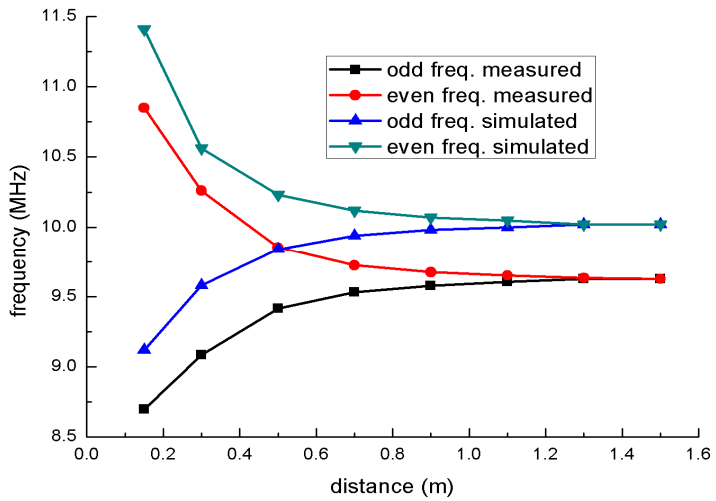

(a)

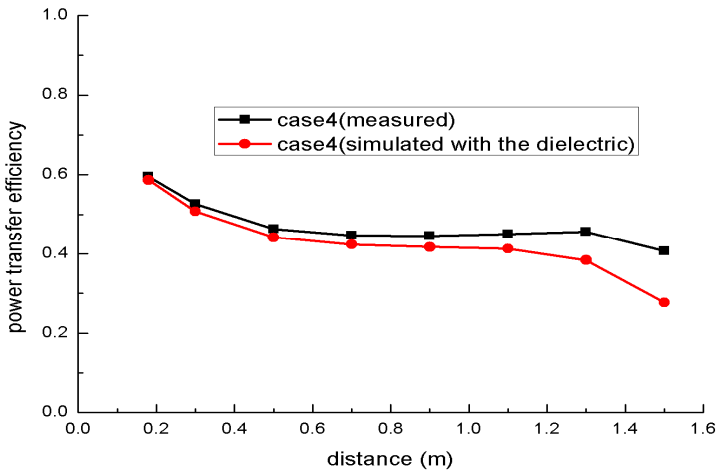

(b)

Fig. 2.9 Comparing the simulation with the measurement: (a) resonant frequency with fixed load impedance (optimum impedance at 1.5 m), (b) power transfer efficiency (loss tan.: 0.009).

2.6 Summary

This paper investigates several adaptive matching methods used to achieve efficient WPT over a near-field region. Although simultaneous conjugate matching demonstrates the best performance, it seems to be very difficult to implement. The performance of the frequency tracking method with a 50 ohm load is nearly the same as that of the simultaneous conjugate matching in the strongly coupled region. However, its transfer efficiency drops drastically as the distance between the two antennas increases beyond the strongly coupled region. We proposed a modified frequency tracking method with a complex load matched at the target distance to achieve a stable efficiency beyond the strongly coupled region. A WPTS using the proposed adaptive matching method was implemented and tested. The experimental results agreed with the theoretical results. It was found that the effect of the dielectric loss of the plastic structure for fixing the antenna should be considered in the WPTS.

Reference

[1] M. Soljacic, “Wireless energy transfer can potentially recharge laptops, cell phones without cords,” Report in San Francisco Massachusetts Institute of Technology, 2006.

[2] A. Kurs, A. Karalis, R. Moffatt, J. D. Joannopoulos, P. Fisher, and M. Soljacic, “Wireless power transfer via strongly coupled magnetic resonances,” *Sciencexpress*, Jun. 7, 2007.

[3] M. Soljacic, E. H. Rafif, and A. Karalis. “Coupled-mode theory for general free-space resonant scattering of waves” *Physical Review*, vol. 75, no.5, pp.1-5, 2007.

[4] A. Karalis, J. D. Joannopoulos, and M. Soljacic, “Efficient wireless non-radiative mid-range energy transfer,” *Annals of Phys*ics, vol. 323, pp.34-48, Jan. 2008.

[5] R. E. Hamam, A. Karalis, J.D. Joannopoulos, and M. Soljacic, “Efficient weakly-radiative wireless energy transfer: An EIT-like approach,” *Annals of Physics*, vol. 324, pp. 1783-1795, Aug. 2009.

[6] Y. Kim and H. Ling, "Investigation of coupled mode behaviour of electrically small meander antennas," *Electron. Lett.*, vol.43, no.23, Nov.

2007.

[7] J. Lee and S. Nam, “Fundamental aspects of near-field coupling antennas for wireless power transfer,” *IEEE Trans. Antennas and Propag*., submitted for publication.

[8] Y. Tak, J. Park, and S. Nam, "Mode-Based Analysis of Resonant Characteristics for Near-Field Coupled Small Antennas," *IEEE Antennas and Wireless Propag. Lett.,* vol. 8, pp. 1238-1241, Nov. 2009.

[9] T.S. Bird, et al., "Antenna impedance matching for maximum power transfer in wireless sensor networks", *IEEE SENSORS 2009*, October 2009, Christchurch, New Zealand, pp. 916-919 .

[10] W. Fu, B. Zhang, and D. Qiu, “Study on frequency-tracking wireless power transfer system by resonant coupling,” *Power Electronics and Motion Control Conf., 2009. IPEMC '09. IEEE 6th International 2009*, pp. 2658 – 2663.

[11] H.A. Haus, Waves and fields in optoelectronics, New Jersey: Prentice-Hall, 1984.

[12] Omnexus website [online]. Available: http://www.omnexus.com/.

Chapter 3

Simple Efficient Resonant Coupling WPTS Operating at Varying Distances between Antennas

3.1 Introduction

Recently many groups have reported on a WPTS that uses resonant coupling [1]-[2]. One of the reported issues is the adaptive matching method when the position of the antennas changes. It is known that the optimum impedance vary drastically with the position of the antennas[2]. However, it is difficult to control the source load impedance simultaneously. The authors of [3]-[5] suggest the frequency tracking method for adaptive matching. By only controlling the frequency of the source of the WPTS, this method achieves almost simultaneous matching conditions in the strong coupling region. However, this method is limited when applied to a

WPTS. In [3]-[5], the operating frequency was shifted about 10 to 20 percent from the center frequency. Generally, the relative bandwidth of industrial, scientific, and medical (ISM) bands are less than 1 percent. Therefore, it is easy to violate the frequency regulation. In this paper, we investigated a novel method that achieves efficient WPT when the operating frequency is fixed and the distance is varied. To do this, the characteristic of the two coupled antennas was analyzed. Then, we took into consideration the types of PA used as a source of the WPTS. The efficiency of PA was analyzed according to the input impedance characteristic of the coupled antennas. Finally, we propose a WPTS, which was verified through experimental results.

3.2 Characteristic of the Two coupled Antennas

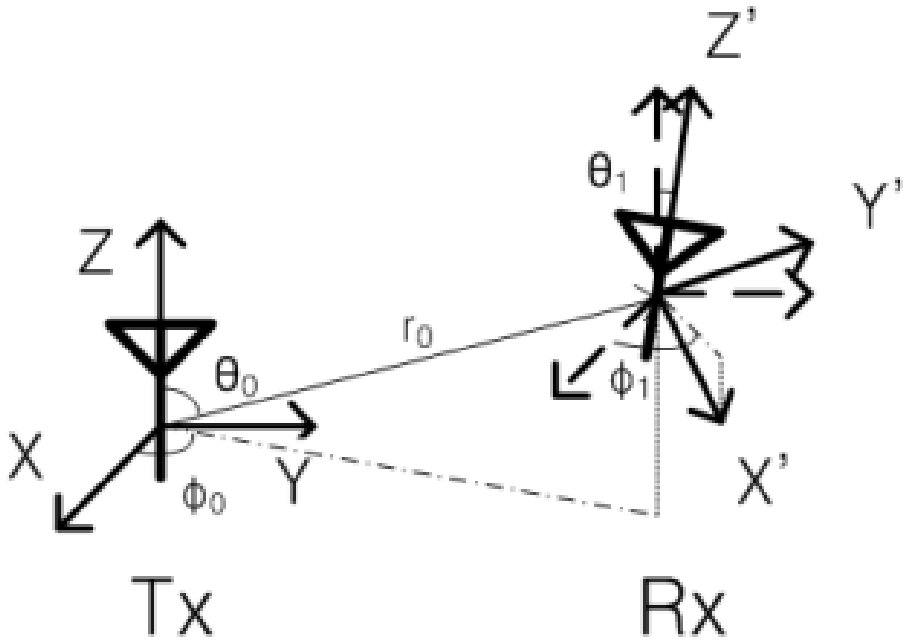

Fig. 3.1 Near-field coupling antennas modeling.

When two resonant antennas are coupled with each other shown in Fig. 3.1, it can be represented in terms of lumped circuit elements. The equivalent circuit model is shown in Fig. 3.2. The transmitting antenna is expressed by R_{Tx}, L_{Tx}, and C_{Tx}. Like the transmitting antenna, the receiving antenna is also expressed by R_{Rx}, L_{Rx}, and C_{Rx}. Additionally, the source resistance is represented by R_S. Generally, a WPTS operates at a very low frequency; therefore, the electrical size of the antennas used with a WPTS is very small.

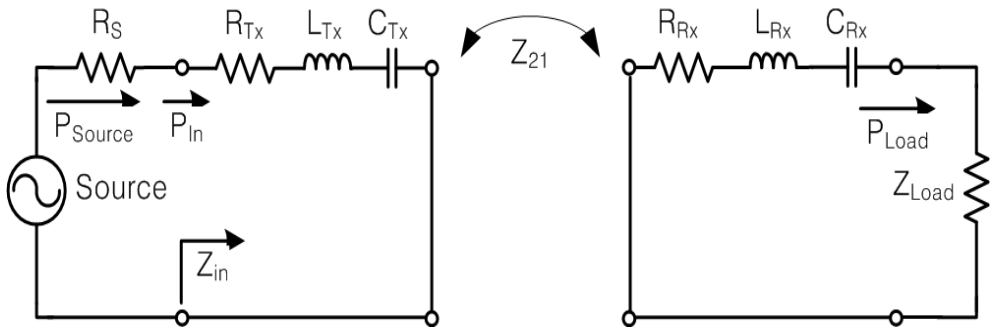

Fig. 3.2 Equivalent circuit of a WPTS.

Thus, we can assume that the antennas used with a WPTS are quasi-canonical minimum scattering (CMS) antenna. A CMS antenna is defined as one that becomes invisible when the antenna port is open-circuited [6]. Hence, we set the Z_{11} and Z_{22} as the impedance of the isolated antennas. In addition, electrically small antennas generate mainly the TE_{10} or TM_{10} spherical modes. Additionally, antennas that generate the same spherical mode are generally used in a WPTS. Thus, in this paper, we assumed that the transmitting and receiving antennas generate a single and identical spherical mode. Generally, a WPTS is used at an electrically close distance. The mutual reactance between the two coupled antennas is dominant compared to the mutual resistance when the antennas are located close enough but are non-touching [2, (56)]. For this reason, the coupling between the antennas is indicated by the mutual reactance X_{21}. In addition, the resonant frequency of the transmitting and

receiving antennas is set at the operating frequency of the WPTS; therefore, the impedance of the antennas can be expressed only by the pure resistance component represented by R_{Tx} and R_{Rx}, respectively. From Fig. 3.2, the power transfer efficiency is defined by

$$\mathrm{PTE} = \frac{P_{Load}}{P_{in}} = \frac{\left|i_{Rx}\right|^2 R_{Load}}{\left|i_{Tx}\right|^2 R_{Tx} + \left|i_{Rx}\right|^2 \left(R_{Rx} + R_{Load}\right)}. \tag{3.1}$$

The relation between the currents of the transmitting and receiving antennas is represented as

$$\frac{i_{Tx}}{i_{Rx}} = \frac{R_{Rx} + R_{Load}}{jX_{21}} \tag{3.2}$$

From (3.1) and (3.2), the power transfer efficiency is represented as

$$\mathrm{PTE} = \frac{1}{\left(1+\frac{R_{Rx}}{R_{Load}}\right)\left(1+\frac{R_{Tx}}{R'_{Load}}\right)} \quad (3.3).$$

R'_{Load} means that the effective load resistance is converted by the mutual impedance. It is represented as

$$R'_{Load} = \frac{\left(X_{21}\right)^2}{R_{Rx}+R_{Load}} \quad (3.4).$$

In addition, the optimum load impedance for the maximum power transfer efficiency is represented as

$$R_{Load}^{opt} = \sqrt{R_{Rx}^2 + \frac{R_{Rx}}{R_{Tx}}\left(X_{21}\right)^2} \quad . \quad (3.5)$$

To maximize the power transfer efficiency, the load resistance must change according to the varied mutual coupling. From (3.3), to maximize the power transfer efficiency, the resistances of the antennas, R_{Tx} and R_{Rx}, have to be relatively very small. The condition of the load resistance and the mutual coupling to maximize the power transfer efficiency is represented as

$$R_{Rx} << R_{Load} << \frac{(X_{21})^2}{R_{Tx}} . \tag{3.6}$$

If R_{Tx} is quite small compared to R'_{Load}, the loss at the transmitting antenna can be ignored. Similarly, if R_{Rx} is quite small compared to R_{Load}, the loss at the receiving antenna can be ignored. Consequently, the network of the two coupled antennas works as a quasi-lossless network.

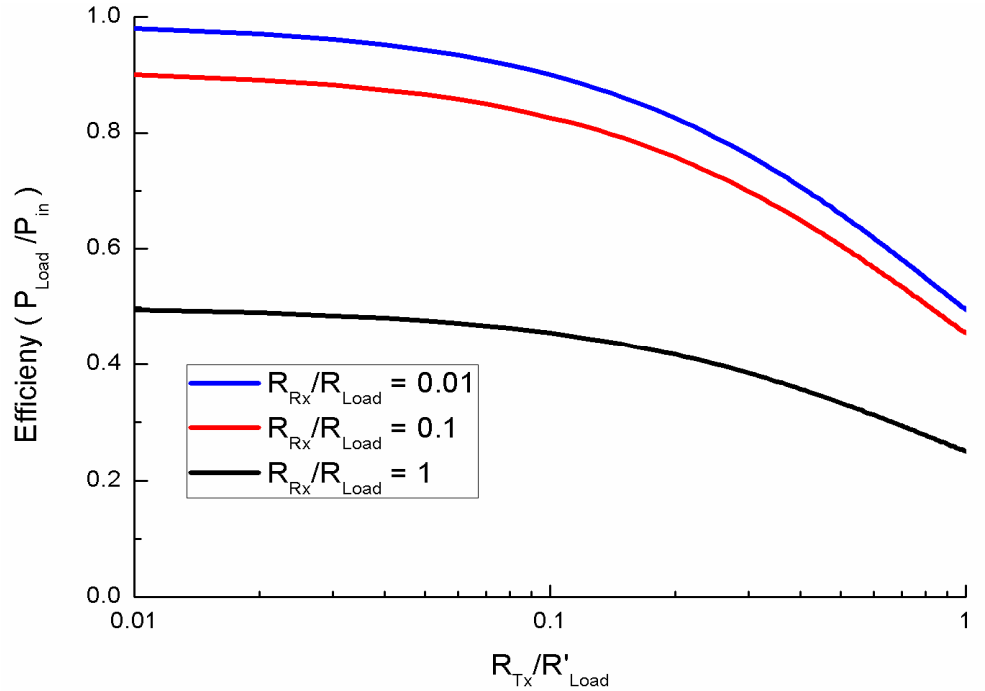

Fig. 3.3 Effect of resistance of antennas and load on the operating power efficiency.

The power transfer efficiency according to the ratio of resistance at the transmitting and receiving antennas is shown in Fig. 3.3. The power transfer efficiency increased when the ratio of resistance decreased. According to the goal of power transfer efficiency, the boundary of the ratio of resistance at both antennas can be suggested. From (3.6), the condition between the resistance of the antennas and the mutual coupling is represented as

$$R_{Tx} \cdot R_{Rx} << \left(X_{21}\right)^2 \tag{3.7}.$$

When the condition of (3.7) is satisfied, the ratio of the resistance is represented as

$$\frac{R_{Rx}}{R_{Load}^{opt}} \approx \frac{R_{Tx}}{\frac{\left(X_{21}\right)^2}{R_{Rx} + R_{Load}^{opt}}}. \tag{3.8}$$

In addition, the maximum efficiency is represented as

$$\mathrm{PTE}_{\max} \approx \frac{1}{\left(1 + \frac{R_{Rx}}{R_{Load}^{opt}}\right)^2} \tag{3.9}.$$

From (3.7), (3.9), and [2, (56)], the maximum electrical distance between the

antennas is represented as

$$kr_0^{\max} = \begin{cases} \sqrt{\left(\frac{1}{\sqrt{\mathrm{PTE}_{\max}}}-1\right)^2 \cdot \eta_{Tx}^{rad} \cdot \eta_{Rx}^{rad} \left[\frac{3}{2}\cos\theta_1\left(3\cos^2\theta_0-1\right)+\frac{9}{4}\sin\theta_1\sin\theta_0\cos\left(\phi_1-\phi_0\right)\right]^2}, & \text{when } \theta_0 \neq \cos^{-1}\left(\frac{1}{\sqrt{3}}\right) \\ \sqrt{\left(\frac{1}{\sqrt{\mathrm{PTE}_{\max}}}-1\right)^2 \cdot \eta_{Tx}^{rad} \cdot \eta_{Rx}^{rad} \left[\frac{9}{4}\sin\theta_1\sin\theta_0\cos\left(\phi_1-\phi_0\right)\right]^2}, & \text{when } \theta_0 = \cos^{-1}\left(\frac{1}{\sqrt{3}}\right) \text{ and } \theta_1 \neq 0 \text{ and } \phi_1-\phi_0 \neq \pm\frac{\pi}{2} \\ \sqrt{\left(\frac{1}{\sqrt{\mathrm{PTE}_{\max}}}-1\right)^2 \cdot \eta_{Tx}^{rad} \cdot \eta_{Rx}^{rad} \left[\frac{3}{2}\cos\theta_1\sin^2\theta_0\right]^2}, & \text{when } \theta_0 = \cos^{-1}\left(\frac{1}{\sqrt{3}}\right) \text{ and } \left(\theta_1 = 0 \text{ or } \phi_1-\phi_0 = \pm\frac{\pi}{2}\right) \end{cases}$$

(3.10)

where η is the radiation efficiency of the antenna. The maximum electrical distance between the antennas is determined by the radiation efficiency of the antennas, the target power transfer efficiency, and the relative location of the receiving antenna. The input resistance at the transmitting antenna is represented as

$$R_{in} = R_{Tx} + \frac{\left(X_{21}\right)^2}{R_{Rx} + R_{Load}} \qquad (3.11).$$

When the distance between the two antennas is varied, the input impedance also changes. Therefore, we need to consider an efficient source type for the WPTS under the condition of varied input impedance.

3.3 Comparison of Source Types

To achieve an efficient WPT system despite the variations in impedance, the characteristic of the PA is such that it is insensitive to load variations. Among various PA types, linear PAs, such as Class-A, B, and AB, have limited efficiency. Thus, nonlinear PAs are preferred in this system due to their high efficiency. In a Class-E PA, the theoretical efficiency is determined by the relationship between the optimum shunt capacitance and load impedance. Thus, the impedance variation can cause sharp degradation in the efficiency [7]. On the contrary, the efficiency of the Class-D PA has a characteristic such that it is insensitive to load variations. The overall efficiency can be sustained over large variations in the load. Therefore, the Class-D PA was selected for the validation of the proposed WPTS. Fig. 3.4 shows the schematic and the efficiency and output power characteristics of the designed class-D amplifier. The input impedance of the measured antenna varied from 4.6 to 400 Ω. It was observed that a high efficiency was maintained over a wide variation in the load resistance.

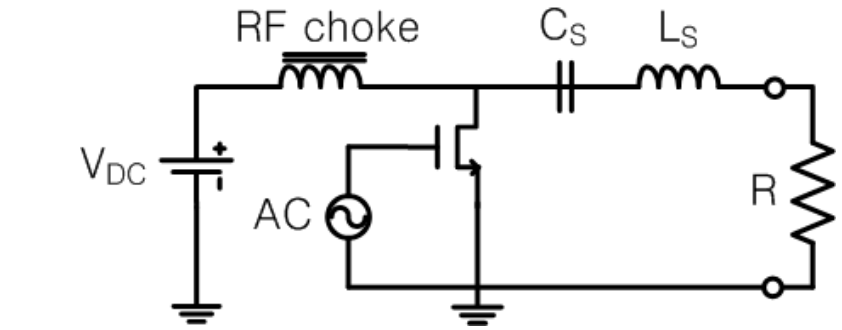

(a)

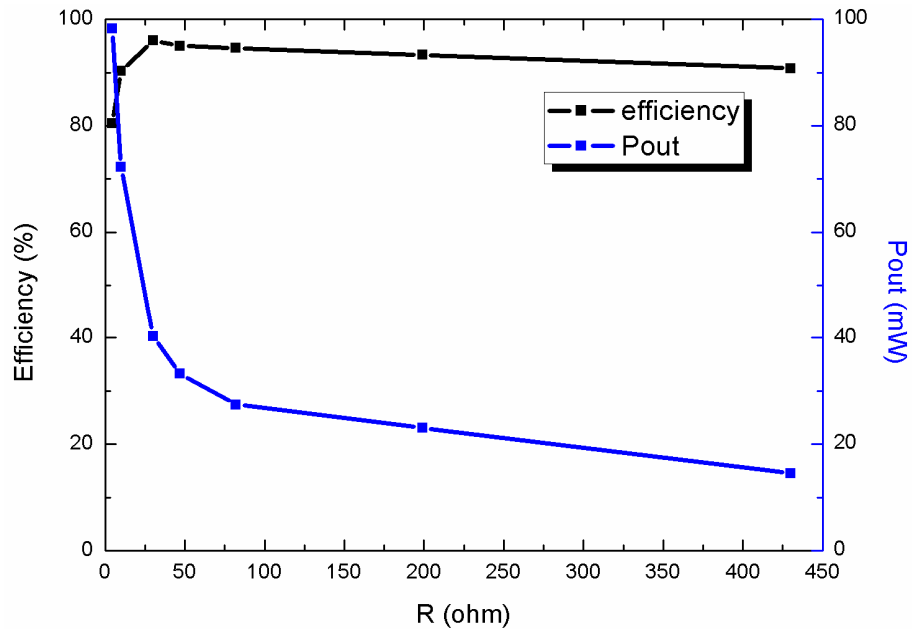

(b)

Fig. 3.4 The schematic, efficiency and output power of PAs against the load resistance: (a) schematic of Class-D PA (V_{DC}=1V, C_S=58pF, L_S=15uH), (b) efficiency and output power.

3.4 Simulation and Measurement

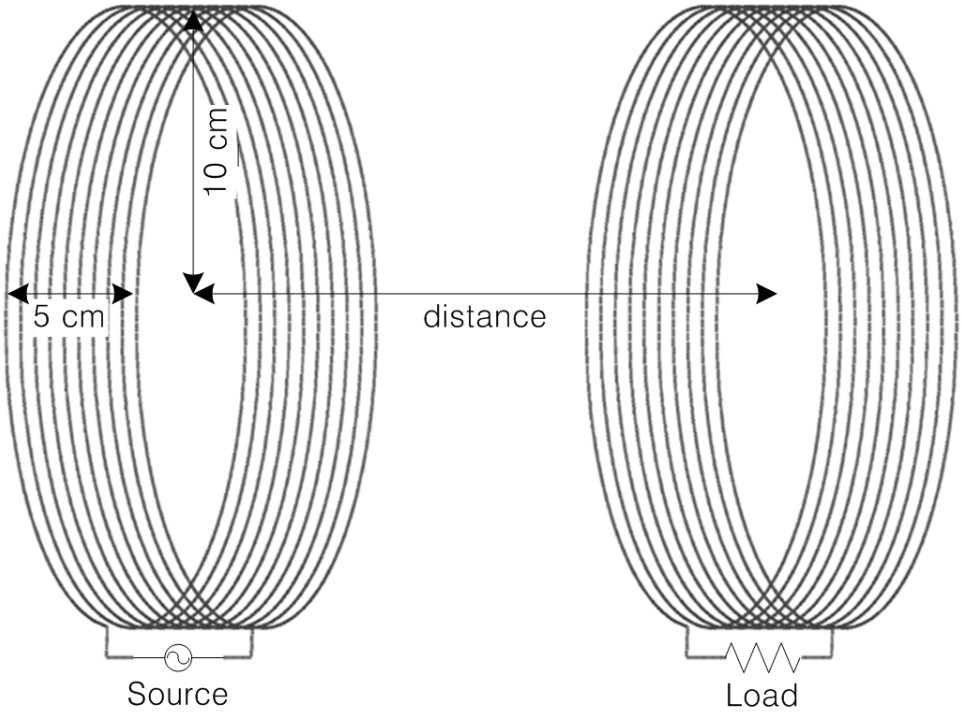

Fig. 3.5 Helix type loop antenna (radius = 10 cm, height = 5 cm, wire thickness = 1 mm, 10 turns, forced resonant frequency = 5.39 MHz).

To verify this theory, we simulated and measured an actual antenna. We used the commercial software package FEKO. We considered a helix-type loop antenna for the simulation and measurements shown in Fig. 3.5. The two antennas were identical. The simulated resistance of the isolated antenna was 4.1 Ω and the

Fig. 3.6 Photograph of the experimental setup of WPTS.

measured resistance of the two isolated antennas was 4.2 and 3.75 Ω, respectively. The radiation efficiency of the antennas was 10-4. A balun efficiency of 95 % was used at each antenna. The transmitting and receiving antenna were collinear. The experimental setup is shown in Fig. 3.6. A Class-D PA was used as the source of this system. The delivered power to the load was measured with an oscilloscope.

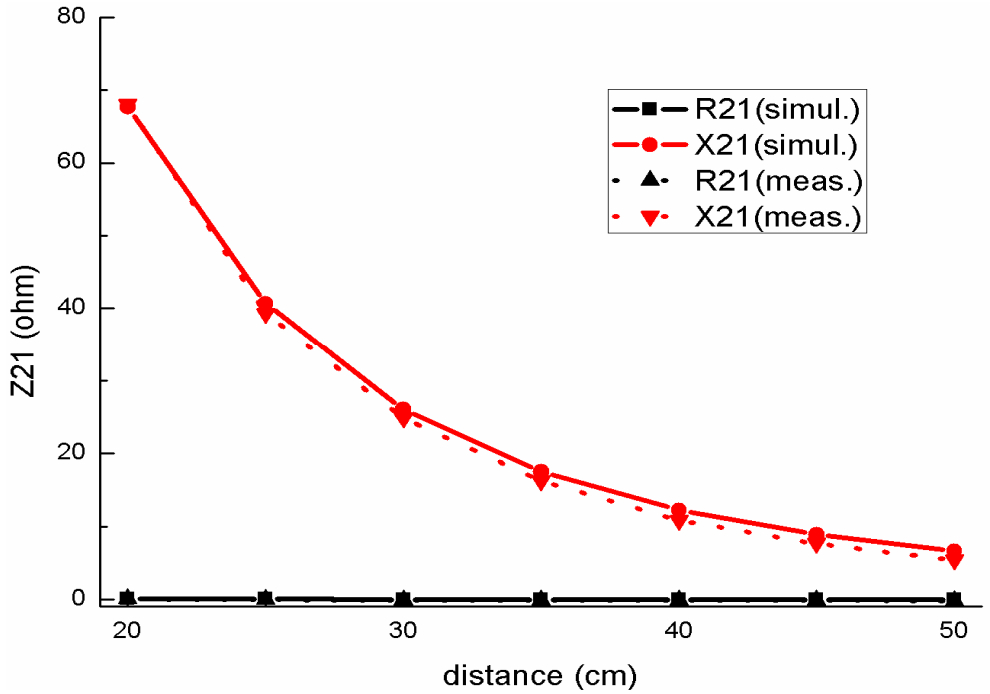

Fig. 3.7 Z_{21} against the distance between the antennas (line: simulated results, dot: measured results).

The simulated and measured mutual impedance is shown in Fig. 3.7. As stated above, the mutual reactance was dominant compared to the mutual resistance. From (3.11) and Fig. 3.7, the smaller the load resistance was, the larger the input resistance was. The simulated and measured total power transfer efficiency is shown in Fig. 8(a). The total power transfer efficiency is represented as

$$\eta_{total} = PTE \cdot \eta_{PA} = \frac{P_{Load}}{P_{Source}} \quad (3.12).$$

From (3.5) and Fig. 3.7, 5 Ω, 25 Ω, and 68 Ω were the optimum load resistance at 20 cm, 30 cm, and 50 cm, respectively. Additionally, only the 25 Ω case satisfied the condition of (3.6) between 20 and 30 cm. From (3.10), the maximum distance, which guarantees a 70 % power transfer efficiency including the balun loss, was about 30 cm.

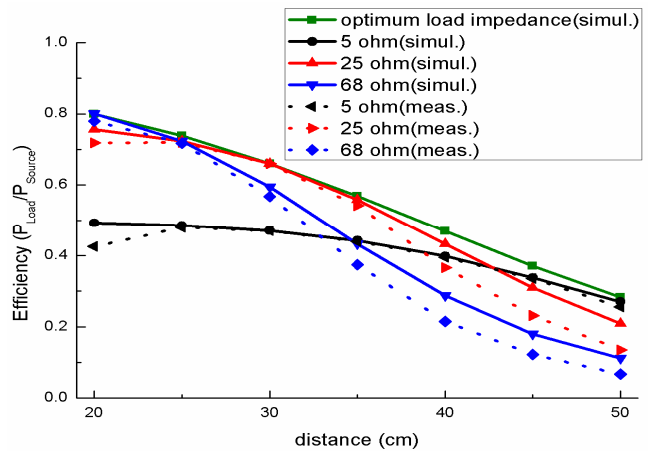

(a)

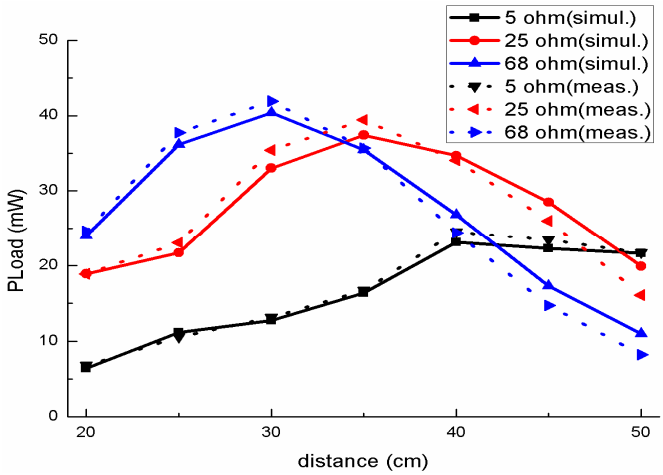

(b)

Fig. 3.8 The total power transfer efficiency and output power for two coupled antennas: (a) comparison of the total power transfer efficiency (line: simulated results including the balun loss and assuming that PA efficiency is 100%, dot: the efficiencies are measured results), (b) output power at the load resistance.

The measured results agreed with the calculated results shown in Fig. 3.8(a). In Fig. 3.8(a), the optimum load impedance case is the maximum power transfer efficiency. When compared with the 5 Ω and 68 Ω cases, the 25 Ω case can efficiently transmit the power at a close distance. There were some differences between the simulated and measured results shown in Fig. 3.8(a). These differences were due to the efficiency of the Class-D PA. From (3.11) and Figs. 3.4 and 3.7, we can infer that the efficiency of the Class-D PA decreases but the output power of the Class-D PA increases when the distance between the antennas is farther apart and the load resistance is bigger. The output power of the Class-D PA and the total power transfer efficiency according to the distance have an opposite trend. The power delivered to the load is shown in Fig. 3.8(b). By only the additional control of the V_{DC} of the Class-D PA can uniform power be transferred to the load. The proposed WPTS grantees 70% system efficiency between 20 and 30 cm.

3.5 Summary

We investigated a method used to achieve efficient WPT over a near-field region when the distance between the antennas varied. First, we analyzed the characteristics of two coupled antennas. Then, the conditions that achieve an efficient WPTS for the load resistance and mutual coupling between the antennas were suggested shown in (3.6). Then, we compared several types of PAs as a source of the WPTS. The Class-D PA has an advantage in regards to the efficiency of the source for a varied load resistance. The efficiency of the proposed system is almost same to that of the optimum load impedance within a range that satisfies the suggested condition. To realize a WPTS when the coupling between two antennas is varied, our proposed system only needed to control the class-D PA and use a proper load resistance, and as a result, mutual coupling was satisfied (3.6). Our method is simple when compared with the conditions of other methods when the operating frequency of the WPTS is fixed. Finally, we implemented and tested the proposed WPTS. The experimental results agreed with the simulation results.

Reference

[1] A. Kurs, A. Karalis, R. Moffatt, J. D. Joannopoulos, P. Fisher, and M. Soljacic, “Wireless power transfer via strongly coupled magnetic resonances,” *Sciencexpress*, Jun. 7, 2007.

[2] J. Lee and S. Nam, “Fundamental aspects of near-field coupling antennas for wireless power transfer,” *IEEE Trans. Antennas and Propag.*, vol. 58, no. 11, pp. 3442-3449, Nov. 2010.

[3] Y. Kim and H. Ling, "Investigation of coupled mode behaviour of electrically small meander antennas," *Electron. Lett.*, vol.43, no.23, Nov. 2007.

[4] A. P. Sample, D. A. Meyer, and J. R. Smith, “Analysis, Experimental Results, and Range Adaptation of Magnetically Coupled Resonators for Wireless Power Transfer,” *IEEE Trans. Industrial Electronics*, vol. 58, pp. 544-554, Feb. 2011.

[5] J. Park, Y. Tak, Y. Kim, Y. Kim and S. Nam, “Investigation of Adaptive Matching Methods for Near Field Wireless Power Transfer,” *IEEE Trans. Antennas and Propag.*, vol. 59, no. 5, May 2011.

[6] W. K. Kahn and H. Kurss, “Minimum-Scattering Antennas,” *IEEE Trans. Antennas and Propag.*, vol. 13, no. 5, pp. 671-675, Sep. 1965.

[7] S. C. Cripps, RF Power Amplifiers for Wireless Communications. London: Artech-House, 2006, p. 180-199

Chapter 4

Analysis of WPT Characteristics for Multiple Receivers by Time Sharing Technique

4.1 Introduction

WPT has been studied for many years [1]. Recently, WPT techniques using resonant coupling has been developed intensively [2]-[5]. The efficiency of the WPTS using near-field coupling is very high at a close range. Many previous work [6]-[9] suggested that the frequency tracking method could be used for adaptive matching. This method controls the frequency of the WPTS source based on the coupling between the antennas. However, the method has various limitations, including the case of multiple receivers charging. To address this issue, we investigated the characteristics of multiple receivers and propose that the time

division WPTS resolves this problem.

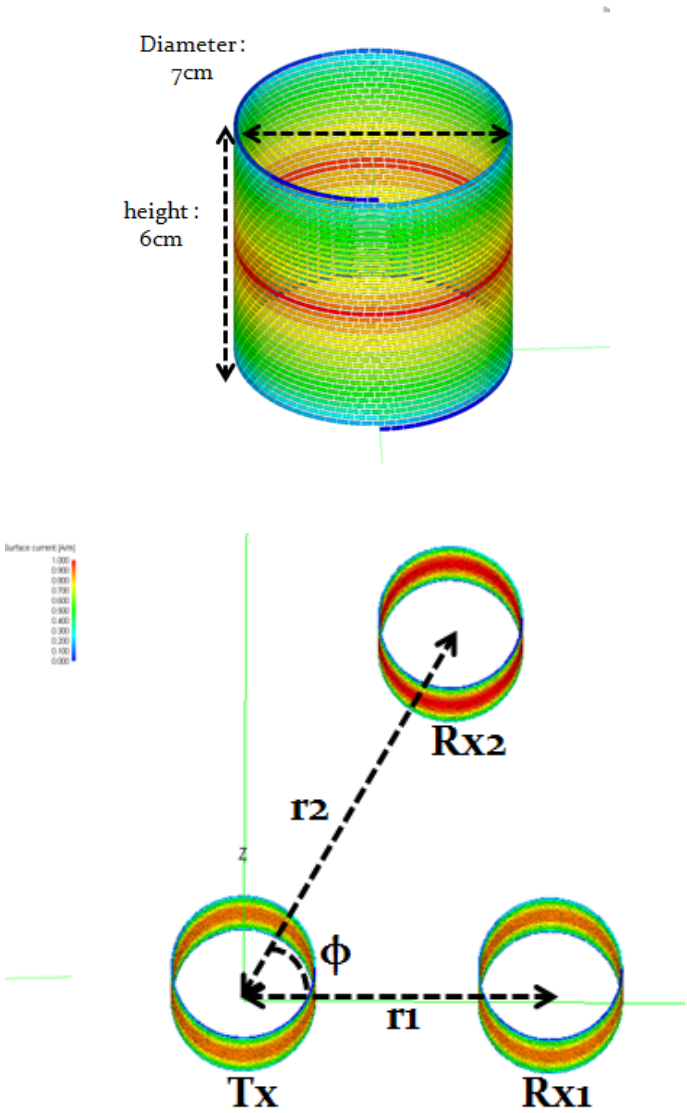

Fig. 4.1. Structure of the multiple receivers charging system

4.2 Frequency Characteristics of Multiple Receivers

The adaptive matching method for WPT using frequency tracking has been studied by many groups. However, the method underlying multiple receivers charging remains unclear. The frequency characteristic of one receiver is greatly different from that of multiple receivers. Figure 4.1 shows the antennas structure and the positions of the multiple receivers. FEKO was used as the simulator. The set-up of the center-fed helical dipole antenna is shown in fig. 4.1. The diameter of the wire was 1 mm, and the height and diameter of the antenna were 6 cm and 7 cm, respectively. The resonant frequency was 13.56 MHz. The distance between the transmitter and the first receiver was fixed at 15 cm. The angle between the transmitter and the receivers was set at 60^{o}. The port impedance at the antennas was 50 Ω. Fig. 4.2 shows the power transfer efficiency (PTE) based on the frequency when the distance between the transmitter and the second receiver was 20 cm. The PTE is defined as:

$$\mathrm{PTE} = \frac{P_L}{P_{avs}} \tag{4.1}$$

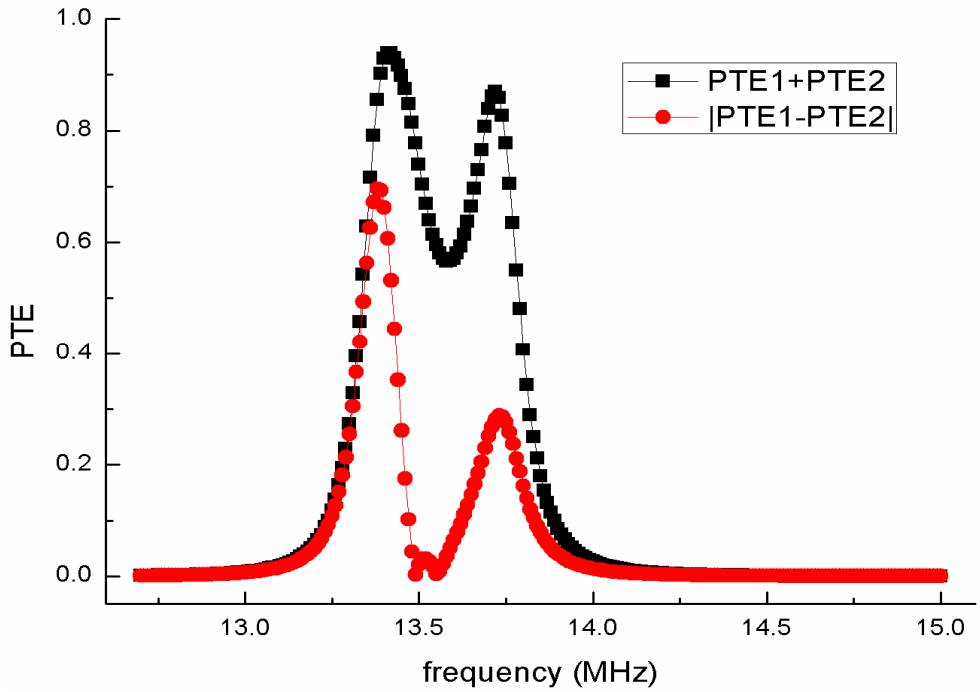

Fig. 4.2. Total power transfer efficiency and the difference between the individual power transfer efficiencies (r_1 = 15 cm, r_2 = 20 cm)

where P_L is the power delivered to the load, P_{avs} is the power available from the source. The total PTE and the difference between the individual power transfer efficiencies are shown in fig. 4.2. Generally, the goal of any power transfer system for multiple receivers is to obtain efficient and equal charging characteristics. At the frequency where the total PTE was efficient, the difference in the PTE of the first and the second receiver was quite high. Therefore, only one of the receivers was

well charged, and the others were hardly charged at all. Although the PTE of the first receiver is high when the second receiver is nonexistent, the almost power from the source is transmitted to the second receiver when the coupling between the source and the second receiver is stronger than the coupling between the source and first receiver. The equal charging characteristics can be realized only under the condition that the couplings are same. Such a situation is not advisable.

4.3 Characteristics of the Time Division WPTS

The analysis at the previous charter highlighted the difficulties surrounding the charging of multiple receivers. To resolve this problem, we propose the time division WPTS. Generally, the WPTS operates at a very low frequency, with the result that the size of the antennas in the system is very small. Therefore, we can assume that an antenna in a WPTS is a quasi-canonical minimum scattering (CMS) antenna. A CMS antenna is defined as one that becomes invisible when the antenna port is open-circuited [10]. Fig. 4.3 shows the proposed circuit of the receiver at the time division WPTS. The switch is added at the port of the receivers. When the switch is off, the load impedance resembles a small capacitor. Therefore, the receiver port is almost open-circuited condition and then the receiver is invisible. As a result, the transmitter can transmit power at the other receiver efficiently.

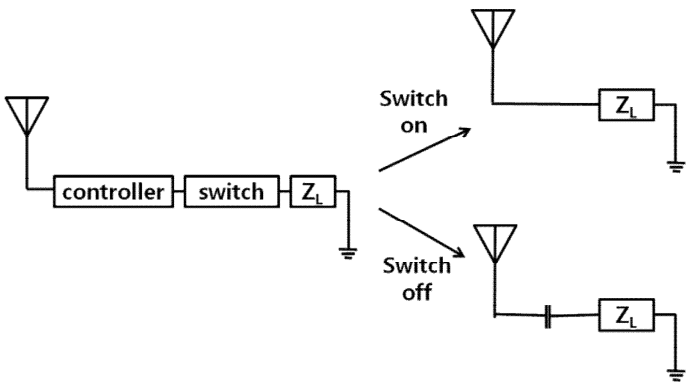

Fig. 4.3. Equivalent circuit of the receiver according to the switch state

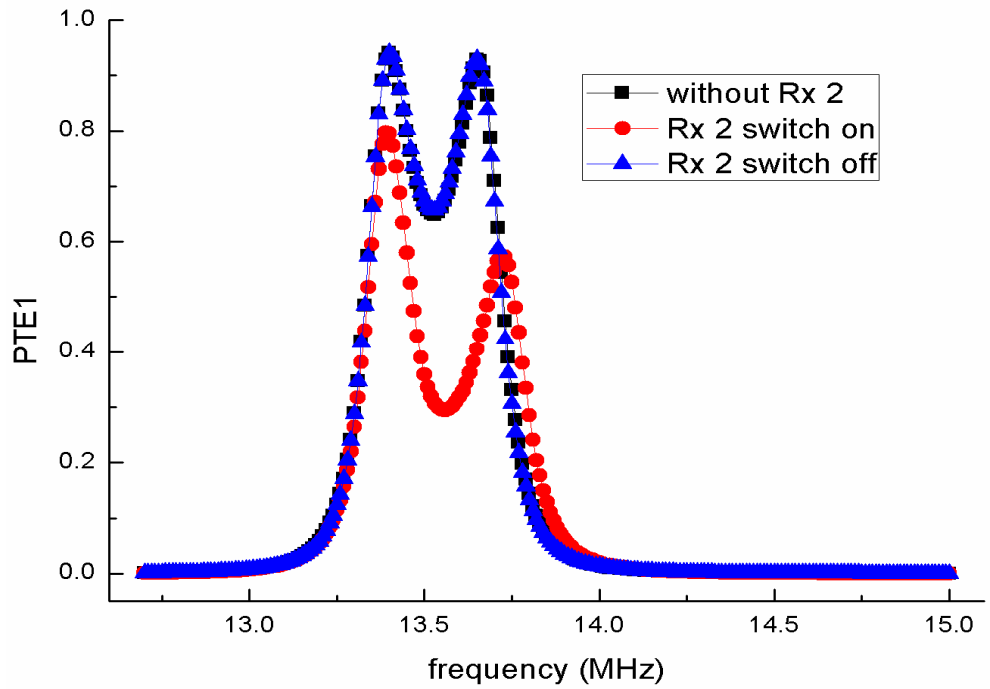

Fig. 4.4. Power transfer efficiency of the first receiver according to the switch state of the second receiver (r_1 = 15 cm, r_2 = 20 cm)

The controller at the receiver controls the switch, which is connected during the allotted time. The PTE of each receiver according to the switch state is shown in figs. 4.4 and 4.5. When the switch of the second receiver was off, the PTE was almost same as that of the case of the without the second receiver as shown in fig. 4.4. Similarly, when the switch of the first receiver was off, the power was efficiently transmitted to the second receiver as shown in fig 4.5.

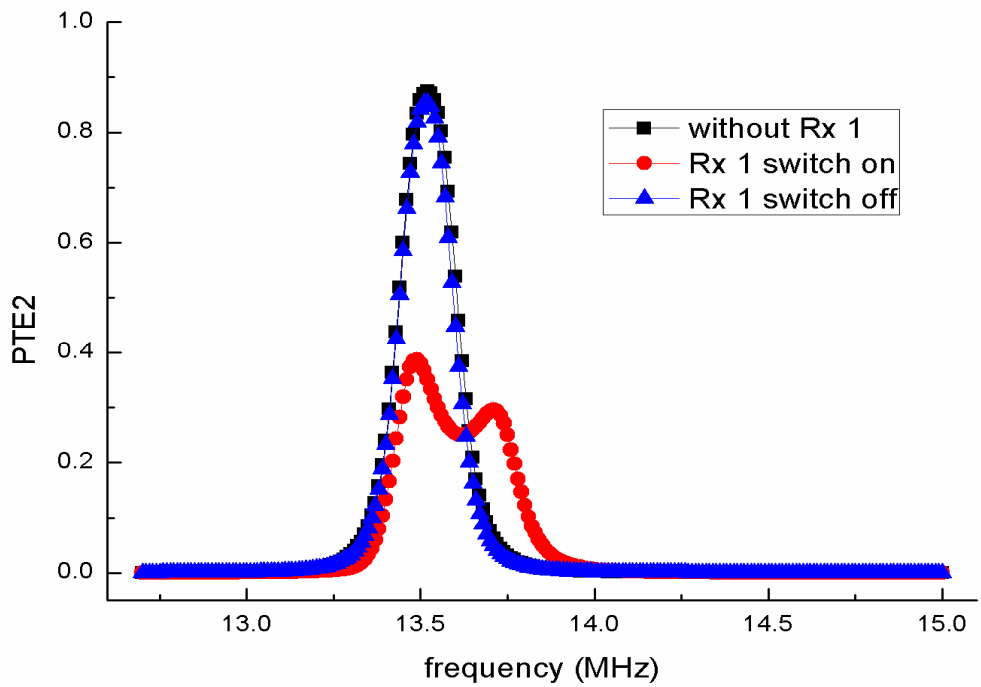

Fig. 4.5. Power transfer efficiency of the second receiver according to the switch state of the first receiver (r_1 = 15 cm, r_2 = 20 cm)

4.4 Summary

In this paper, the characteristics of the WPTS to charge the multiple receiver is analyzed. When multiple receiver are charged, to achieve efficiently charging and equally charging at the same time is difficult. So we propose a time division technique to use a characteristic of CMS antenna. By control of switches of receiver, we can make a condition of single receiver. We conclude that in terms of multiple receiver' charging, the proposed time division WPTS can transmit power efficiently and equally.

Reference

[1] N. Tesla, “Apparatus for transmitting electrical energy,” U.S. Patent 1 119 732, Dec. 1, 1914.

[2] A. Kurs, A. Karalis, R. Moffatt, J. D. Joannopoulos, P. Fisher, and M. Soljacic, “Wireless power transfer via strongly coupled magnetic resonances,” *Sciencexpress*, Jun. 7, 2007

[3] J. Lee and S. Nam, “Fundamental aspects of near-field coupling antennas for wireless power transfer,” *IEEE Trans. Antennas and Propag.*, vol. 58, no. 11, pp. 3442-3449, Nov. 2010.

[4] G. Kim, Y. Jung and B. Lee, “Wireless Power Transmission between Two Metamaterial-Inspired Loops at 300 MHz,” *Journal of Korean Institute Electronic Engineering and Science*, vol. 10, no. 4, Dec. 2010.

[5] I. Awai and T. Ishida, “Design of Resonator-Coupled Wireless Power Transfer System by Use of BPF Theory,” *Journal of Korean Institute Electronic Engineering and Science*, vol. 10, no. 4, Dec. 2010.

[6] Y. Kim and H. Ling, “Investigation of coupled mode behaviour of electrically small meander antennas,” *Electron. Lett.*, vol. 43, no. 23, Nov. 2007.

[7] W. Fu, B. Zhang, and D. Qiu, “Study on frequency-tracking wireless power transfer system by resonant coupling,” *Power Electronics and Motion Control Conf., 2009. IPEMC '09. IEEE 6th International 2009*, pp. 2658–

2663.

[8] A. P. Sample, D. A. Meyer, and J. R. Smith, “Analysis, Experimental Results, and Range Adaptation of Magnetically Coupled Resonators for Wireless Power Transfer,” *IEEE Trans. Industrial Electronics*, vol. 58, pp. 544-554, Feb. 2011.

[9] J. Park, Y. Tak, Y. Kim, Y. Kim, and S. Nam, “Investigation of Adaptive Matching Methods for Near Field Wireless Power Transfer,” *IEEE Trans. Antennas and Propag.*, vol. 59, no. 5, May 2011.

[10] W. K. Kahn and H. Kurss, “Minimum-Scattering Antennas,” *IEEE Trans. Antennas and Propag.*, vol. 13, no. 5, pp. 671-675, Sep. 1965.

Chapter 5

Investigation of the Effect of Surroundings using Characteristic Mode Method for WPT

5.1 Introduction

The characteristic mode (CM) method is well known for the ability to provide a series of fundamental modes for arbitrarily shaped conducting bodies, regardless of the feeding methods. Theory of the CM method was established by Harrington and Mautz in the 1970s, in which the electric field integral operator is used to connect the electric field intensity and surface current [1], [2]. The characteristic values and characteristic currents are obtained through solving the generalized eigenvalue operator equations. During the past years, the CM method is widely used in the synthesis and optimization of various antennas and scatters [3]–[5].

The CM method is usually combined with the method of moments (MoM) by dividing the complex regions into many small meshes [2], and the characteristic

modes are incorporated in the solutions of generalized eigenvalue matrix equations. The characteristic currents are the linear superposition of the surface current components on all the meshes, and obviously much information is still hidden in various figures or data sheets. Very few attempts for the exact or closed-form models of the characteristic currents were reported in the literature.

To realize the WPTS, many important issues for WPT remain unsolved. One of the important issue is the effect of the surroundings for WPTS. In this paper, we investigate the effect of the surroundings using characteristic mode method. When finite size of the metal plate exist near WPTS, the scattering field by the metal plate is analyzed using characteristic mode method.

5.2 Characteristic Currents

Consider the problem of one or more conducting bodies, defined by the surface S, in an impressed electric field E^i. An operator equation for the current J on S is

$$\left[L(J) - E^i \right]_{\tan} = 0 \qquad (5.1).$$

Physically, L(J) gives the electric intensity E at any point in space due to the current J on S. The operator appearing in (5.1) has the dimensions of impedance as

$$Z(J) = R(J) + jX(J) = \left[L(J) \right]_{\tan} \qquad (5.2)$$

where R and X are the real and imaginary parts of the impedance operator. Characteristic modes or characteristic currents can be obtained as the eigenfunctions of the following particular weighted eigenvalue equation:

$$X\left(J_n\right)=\lambda_n R\left(J_n\right) \tag{5.3}$$

where the λ_n are the eigenvalues, the J_n are the eigenvectors or characteristic currents. This impedance operator is obtained after formulating an integro differential equation. It is known from the reciprocity theorem that if Z is a linear symmetric operator, then, its Hermitian parts, R and X, will be real and symmetric operators. From this, it follows that all eigenvalues λ_n in Equation (5.3) are real, and all the characteristic currents, J_n can be chosen real or equiphasal [a complex constant times a real function] over the surface on which they are defined [1]. Moreover, the choice of R as a weight operator in Equation (5.3) is responsible for the orthogonality properties of characteristic modes described in [1], which can be summarized as

$$\left\langle J_m, RJ_n\right\rangle=\left\langle J_m^*, RJ_n\right\rangle=\delta_{mn} \tag{5.4}$$

$$\left\langle J_m, XJ_n\right\rangle=\left\langle J_m^*, XJ_n\right\rangle=\lambda_n\delta_{mn} \tag{5.5}$$

where δ_{mn}, is the Kronecker delta (1 if m=n else 0). The characteristic currents are of indeterminate amplitude. So each characteristic current can be normalized the radiating power.

Consistent with Equation (5.3), the characteristic modes J_n can be defined as the real currents on the surface of a conducting body that only depend on its shape and size, and are independent of any specific source or excitation. In practice, to compute characteristic modes of a particular conducting body, Equation (5.3) needs to be reduced to matrix form, as explained in [2], using a Galerkin formulation [6]:

$$[X]J_n = \lambda_n [R]J_n \tag{5.6}$$

Next, eigenvectors, J_n and eigenvalues, λ_n of the object are obtained by solving the generalized eigenproblem of Equation (5.6).

5.3 Modal solutions

A modal solution for the current J on a conducting body can be obtained by using the characteristic currents as both expansion and testing functions in the method of moments [6]. Following this procedure, we assume J to be a linear superposition of the mode currents

$$J = \sum_n \alpha_n J_n \tag{5.7}$$

where the α_n are coefficients to be determined. Substituting (5.7) into the operator equation (5.l), and using the linearity of L, we obtain

$$\left[\sum_n \alpha_n L J_n - E^i \right]_{\tan} = 0 \tag{5.8}$$

Next, the inner product of (5.8) with each J_m, in turn is taken, giving the set of equations

$$\sum_n \alpha_n \langle J_m, ZJ_n \rangle - \langle J_m, E^i \rangle = 0 \qquad (5.9).$$

Here we have put $L_{tan} = Z$, and dropped the subscript "tan" on E^i. Because of the orthogonality relationship (5.4), (5.5), (5.9) reduces to

$$\alpha_n (1 + j\lambda_n) = \langle J_n, E^i \rangle \qquad (5.10)$$

The right-hand side of (5.10) is called the modal excitation coefficient:

$$V_n^i = \langle J_n, E^i \rangle = \oiint_S J_n \cdot E^i ds \qquad (5.11)$$

Substituting for α_n from (5.10) into (5.7), we have the modal solution for the current J on S:

$$J = \sum_n \frac{V_n^i}{1 + j\lambda_n} \frac{J_n}{\langle J_n, RJ_n \rangle} \tag{5.12}.$$

5.4 Modified Z-matrix

The effect of the surroundings for WPTS can be expressed in matrix form as (5.13) using kirchhoff's voltage law. Z_{Tx} and Z_{Rx} are impedance of the isolated transmitting and receiving antenna, respectively. Φ_{α_β} means the magnetic flux, which pass through α antenna, occurred by β current. PEC_{Tx} and PEC_{Rx} is the current at the PEC plate occurred by the transmitting and receiving antenna, respectively. The current at the antennas set up a unit current.

$$\begin{bmatrix} V_s \\ 0 \end{bmatrix} = \begin{bmatrix} Z_{Tx} + j\omega\left(\Phi_{Tx\_PEC_{Tx}}\right) & j\omega\left(\Phi_{Tx\_Rx} + \Phi_{Tx\_PEC_{Rx}}\right) \\ j\omega\left(\Phi_{Rx\_Tx} + \Phi_{Rx\_PEC_{Tx}}\right) & Z_{R2} + Z_{Load} + j\omega\left(\Phi_{Rx\_PEC_{Rx}}\right) \end{bmatrix} \begin{bmatrix} I_{Tx} \\ I_{Rx} \end{bmatrix} \quad (5.13)$$

The flux is represented as

$$\Phi_{Tx\_Rx} = \int_{S_{Tx}} B_{Rx} \bullet dS_{Tx} = \oint_{C_{Tx}} A_{Rx} \bullet dl_{Tx} = \frac{\mu_0}{4\pi} \oint_{C_{Tx}} \oint_{C_{Rx}} \frac{e^{-jkR}}{R} dl_{Tx} \bullet dl_{Rx}$$

$$\Phi_{Tx\_PEC_{Tx}} = \int_{S_{Tx}} B_{PEC_{Tx}} \bullet dS_{Tx} = \oint_{C_{Tx}} A_{PEC_{Tx}} \bullet dl_{Tx} = \frac{\mu_0}{4\pi} \oint_{C_{Tx}} \iint_{S_{PEC}} \frac{e^{-jkR} J_{S\_PEC_{Tx}}}{R} dS_{PEC} \bullet dl_{Tx}$$

$$\Phi_{Tx\_PEC_{Rx}} = \int_{S_{Tx}} B_{PEC_{Rx}} \bullet dS_{Tx} = \oint_{C_{Tx}} A_{PEC_{Rx}} \bullet dl_{Tx} = \frac{\mu_0}{4\pi} \oint_{C_{Tx}} \iint_{S_{PEC}} \frac{e^{-jkR} J_{S\_PEC_{Rx}}}{R} dS_{PEC} \bullet dl_{Tx}$$

$$\Phi_{Rx\_Tx} = \int_{S_{Rx}} B_{Tx} \bullet dS_{Rx} = \oint_{C_{Rx}} A_{Tx} \bullet dl_{Rx} = \frac{\mu_0}{4\pi} \oint_{C_{Rx}} \oint_{C_{Tx}} \frac{e^{-jkR}}{R} dl_{Rx} \bullet dl_{Tx}$$

$$\Phi_{Rx\_PEC_{Tx}} = \int_{S_{Rx}} B_{PEC_{Tx}} \bullet dS_{Rx} = \oint_{C_{Rx}} A_{PEC_{Tx}} \bullet dl_{Rx} = \frac{\mu_0}{4\pi} \oint_{C_{Rx}} \iint_{S_{PEC}} \frac{e^{-jkR} J_{S\_PEC_{Tx}}}{R} dS_{PEC} \bullet dl_{Rx}$$

$$\Phi_{Rx\_PEC_{Rx}} = \int_{S_{Rx}} B_{PEC_{Rx}} \bullet dS_{Rx} = \oint_{C_{Rx}} A_{PEC_{Rx}} \bullet dl_{Rx} = \frac{\mu_0}{4\pi} \oint_{C_{Rx}} \iint_{S_{PEC}} \frac{e^{-jkR} J_{S\_PEC_{Rx}}}{R} dS_{PEC} \bullet dl_{Rx}$$

(5.14).

Here R denotes a distance between a source and a field point. $J_{S\_PEC\alpha}$ means the surface current occurred by α antenna field on the surface of metal plate. The surface current on the metal plate is calculated using characteristic mode method (5.12). From the Z-matrix, the maximum power efficiency and the optimum load impedance can be find. The input impedance of the transmitting antenna is represented as

$$Z_{in} = Z_{11} - \frac{Z_{21}^{\ 2}}{Z_{22} + Z_{load}} \tag{5.15}$$

where Z_{load} is the load impedance of the receiving antenna. The power transfer efficiency is defined by

$$PTE = \frac{P_{load}}{P_{in}} = \frac{\mathrm{Re}\left[Z_{load}\right]}{\mathrm{Re}\left[Z_{in}\right]}\left|\frac{Z_{21}}{Z_{22}+Z_{load}}\right|^2 \quad (5.16).$$

The optimum load impedance to maximize the power transfer efficiency can be yielded as

$$\frac{\partial PTE}{\partial \mathrm{Re}\left[Z_{load}\right]} = 0, \ \frac{\partial PTE}{\partial \mathrm{Im}\left[Z_{load}\right]} = 0 \quad (5.17).$$

From (5.16)-(5.17), the optimum load impedance condition is represented as

$$\begin{aligned}\mathrm{Re}\left[Z_{load}^{opt}\right] &= \mathrm{Re}\left[Z_{22}\right]\sqrt{1-\mathrm{Re}\left[T^2\right]-\frac{\mathrm{Im}\left[T^2\right]^2}{4}} \\ \mathrm{Im}\left[Z_{load}^{opt}\right] &= \frac{\mathrm{Re}\left[Z_{22}\right]}{2}\mathrm{Im}\left[T^2\right]-\mathrm{Im}\left[Z_{22}\right]\end{aligned} \tag{5.18}$$

where $T = Z_{21}/\sqrt{\mathrm{Re}\left[Z_{11}\right]\mathrm{Re}\left[Z_{22}\right]}$. Substituting (5.18) into the power transfer efficiency equation (5.16), we obtain the maximum power transfer efficiency as

$$PTE^{\max} = \frac{\left|T\right|^2}{2-\mathrm{Re}\left[T^2\right]+\sqrt{4-4\,\mathrm{Re}\left[T^2\right]-\mathrm{Im}\left[T^2\right]^2}} \tag{5.19}.$$

5.5 Example

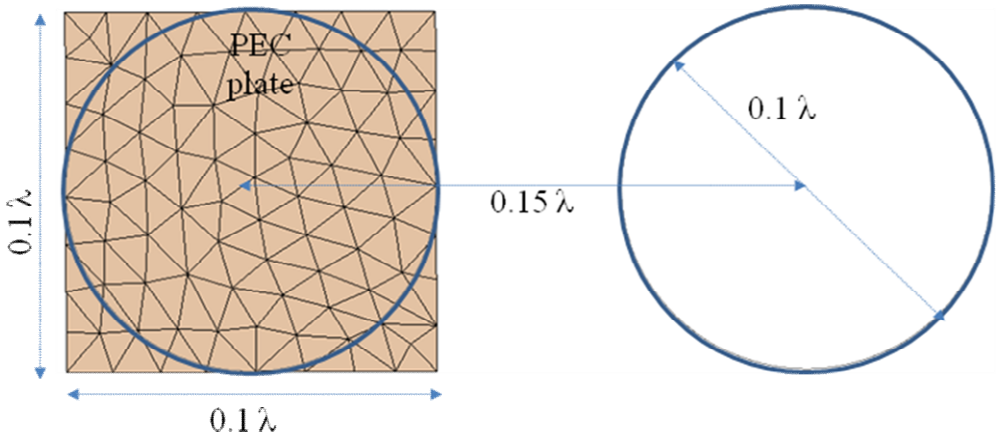

Fig. 5.1 Small loop antenna with PEC plate (diameter = 0.1 λ, distance between antennas = 0.15 λ, PEC plate = 0.1 x 0.1 λ^2).

To verify the theory, we compare the Z-matrix of an actual antenna with that in (5.13). A small loop antenna at which uniform current flow is chosen as illustrated in Fig. 5.1. The diameter of a loop antenna is 0.1 λ, the size of PEC plate is 1 by 1 λ^2, and the distance between loop antennas is 0.15 λ. Material of loop antennas is copper and diameter of wire is 1 mm. Length of a loop antenna is about 0.314 λ. Because the length is not small as compared with wavelength, the current at the loop antenna is not uniform. So we complement series capacitances to prevent a change of phase. Three capacitances of 2.2 pF are used.

To apply characteristic mode method, the impedance matrix of the PEC plate is required. The matrix were obtained by a simulation using FEKO, a commercially available software. From general eigenvalue equation (5.3), characteristic modes and eigenvalues of the PEC plate are obtained. Fig. 5.2 illustrates the current distribution for the first six eigenvectors of a PEC plate. Computation of these characteristic currents was done using 191 Rao-Wilton-Glisson (RWG) basis functions for expansion and testing. In addition, for a better understanding, Fig. 5.3 shows current schematics of these six characteristic modes. Mode current 1, 2, 4 and 5 present capacitive nature due to its currents forming opened lines. On the other hand, mode current 3 and 6 depict inductive nature due to its currents forming closed loops over the plate. Eigenvalues of the six characteristic current mode are shown in TABLE 5.1.

TABLE 5.1

EIGENVALUES OF SIX CHARACTERISTIC CURRENT

Mode	Eigenvalue (λ)
1	-7.33 E1
2	-7.36 E1
3	1.93 E2
4	-1.04 E4
5	-2.48 E4
6	7.60 E4

Magnitude of Eigenvalues gives information about how well the associated mode radiates. In contrast, reactive power is proportional to the magnitude of the eigenvalue. The sign of the eigenvalue determines whether the mode contributes to storing magnetic energy or electric energy. As shown in TABLE 5.1, characteristic modes 3 and 6 are plus sign eigenvalues. So the currents characteristic are inductively. While characteristic modes 1,2,4 and 5 are minus sign eigenvalues. So the currents characteristic are capacitively as shown in Fig. 5.2 and Fig. 5.3.

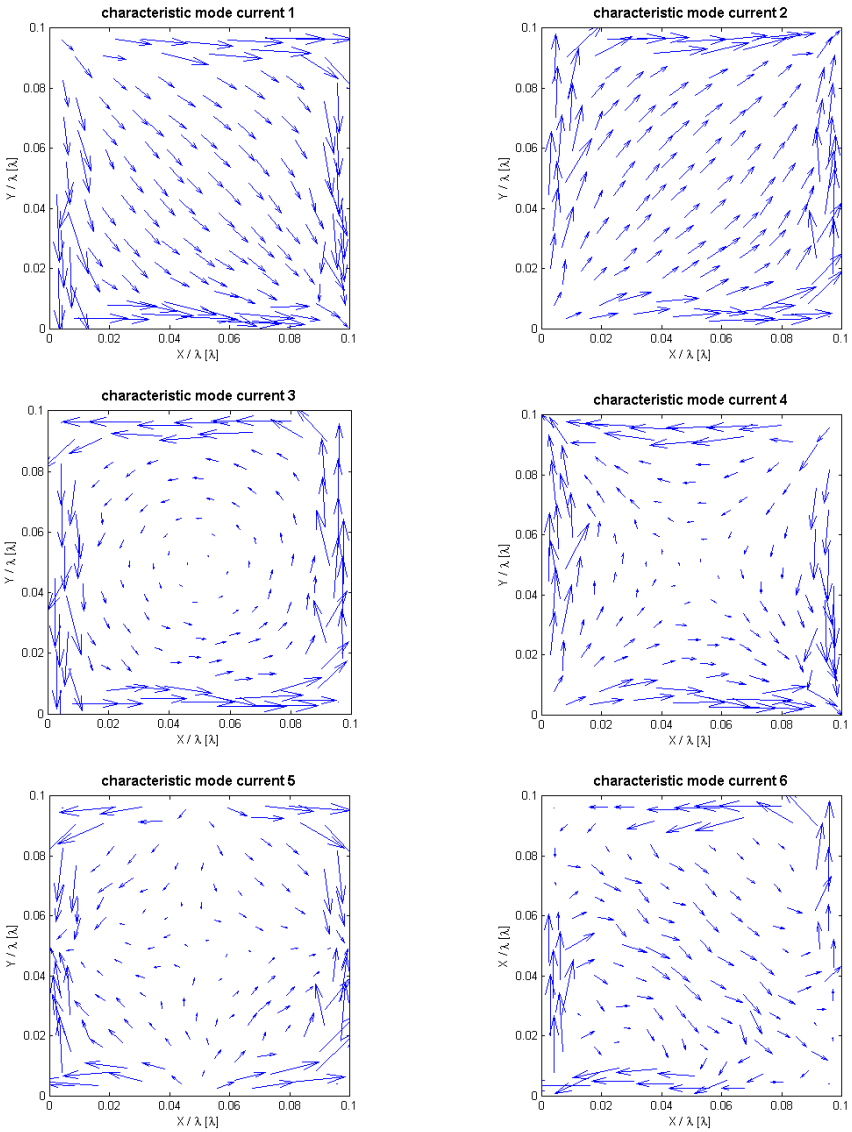

Fig. 5.2 Current distribution for the first six eigenvectors of a PEC plate

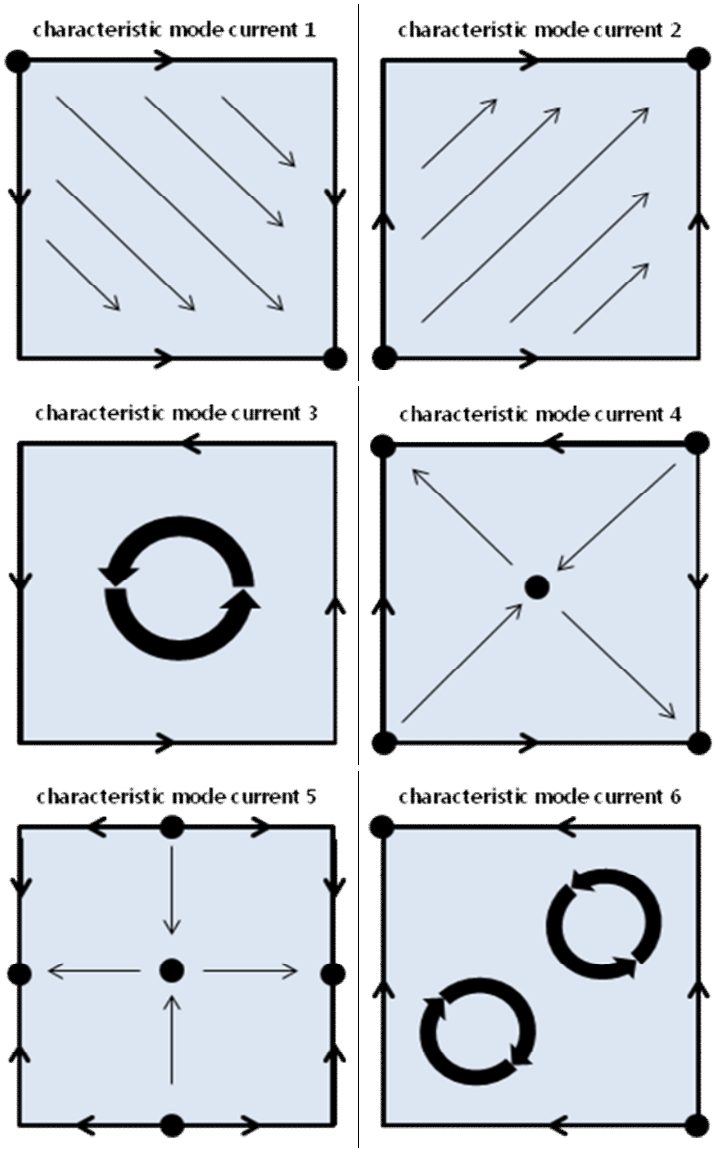

Fig. 5.3 Current schematics for the first six eigenvectors of a PEC plate

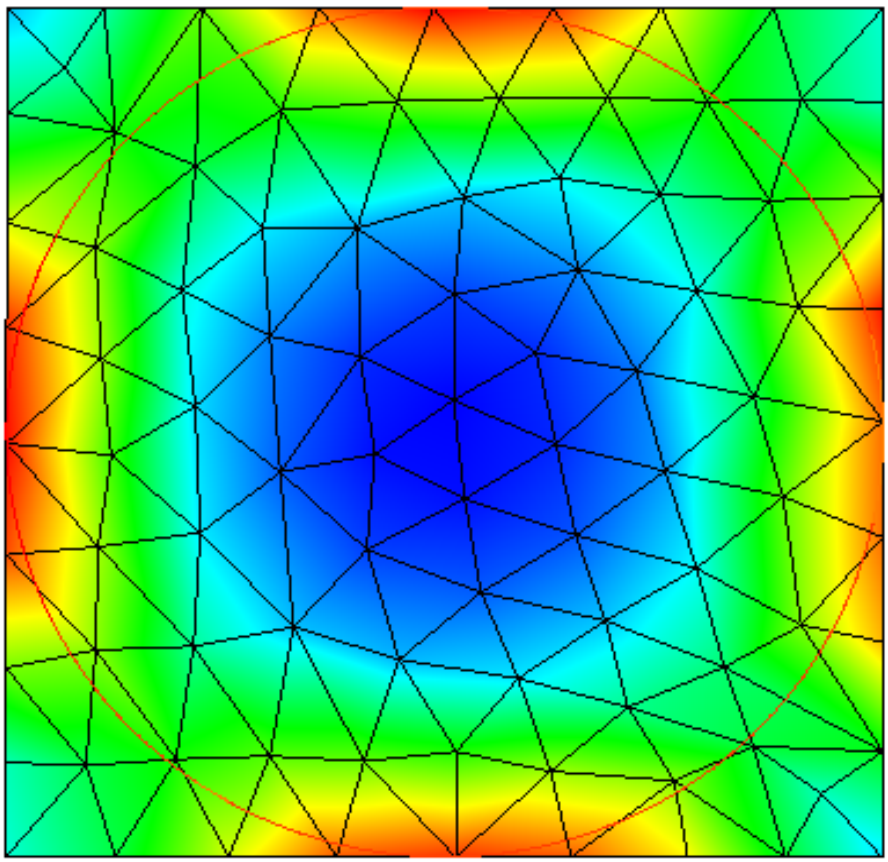

Fig. 5.4 Current distribution on PEC plate induced by small loop antenna.

Current distribution at the PEC plate induced by small loop antenna is shown in Fig. 5.4. The height of the antenna from PEC plate is varied in 0.001 ~ 0.015 λ. In this simulation condition, the current distribution is unchanged according to the

height. Only amplitude of the current varies as the height of an antenna. Also, the current form is very similar with third characteristic mode current distribution. We can predict that the effect of PEC plate can obtain using one characteristic mode in this simulation condition.

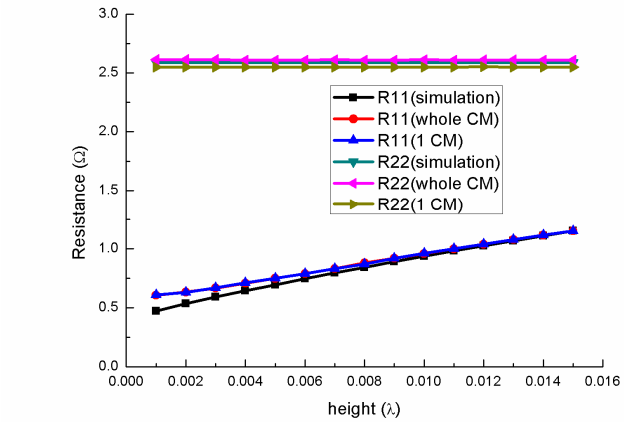

(a)

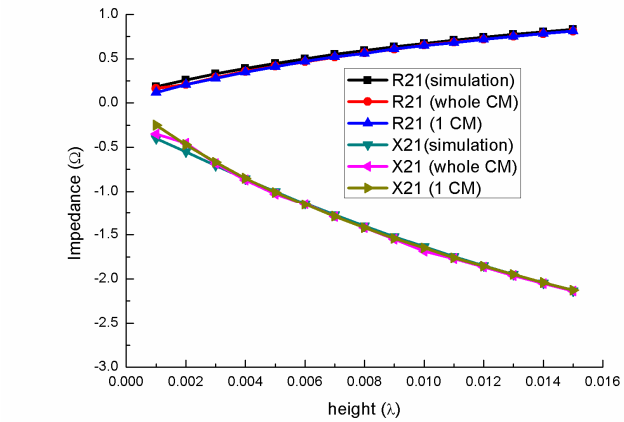

(b)

Fig. 5.5 Z-parameter of the coupled loop antennas with PEC plate according to the height of loop antenna: (a) real component of Z_{11} and Z_{22}, (b) Z_{21} (CM: characteristic Mode)

From (5.19), the power transfer efficiency relate with real component of Z_{11} and Z_{22} and Z_{21} parameter. Impedance of isolated loop antenna is calculated as

$$Z_{loop} = 20\pi^2\left(\frac{2\pi a}{\lambda}\right)^4 + \frac{a}{w}\sqrt{\frac{\pi f \mu}{\sigma}} + j2\pi f \mu a\left(\log\left(\frac{8a}{w}\right) - 2\right) \qquad (5.20)$$

where a is radius of a loop, w is radius of wire, σ is conductivity. From (5.14), (5.20), the Z-matrix (5.13) can be calculated. Fig. 5.5(a) shows the real component of Z_{11} and Z_{22} according to the height of the antenna. Because of the coupling between the transmitting small loop antenna and PEC plate the real component of Z_{11} is changed according to the height of the antenna. Because the field of the loop antenna cancel out by the current at the PEC plate, the radiation resistance of the loop antenna is also decrease by the effect of PEC plate. So the more coupling, the more decrease of the real component of Z_{11} as shown in Fig. 5.5(a). But the real component of Z_{22} is unchanged since the effect of PEC plate is week in receiving antenna. Fig. 5.5(b) shows the real and imaginary component of

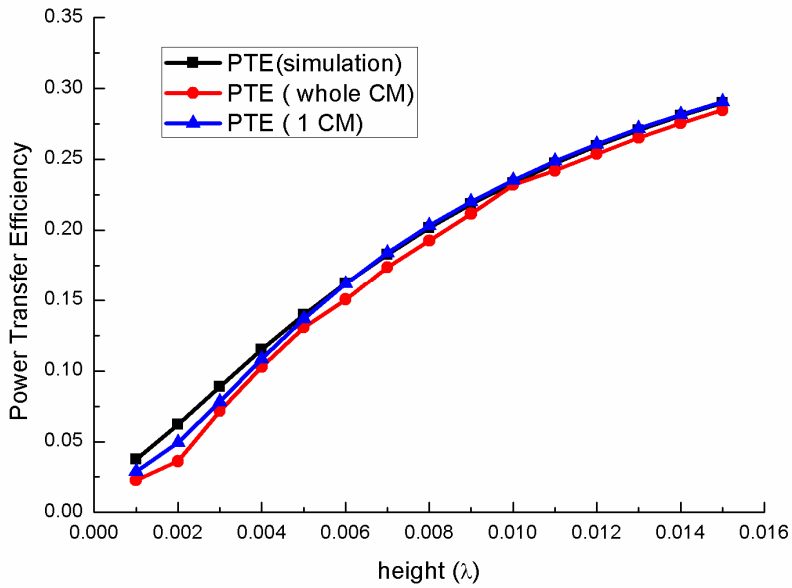

Fig. 5.6 Power transfer efficiency with PEC plate.

Z_{21}. The current on PEC plate is counter to the current of transmitting antenna. When the height between PEC plate and transmitting antenna is closer, the coupling between the loop antennas is weaker. The results agree with the calculation results using characteristic modes. Fig. 5.6 shows the power transfer efficiency with PEC plate. From (5.19) and fig. 5.5, we can predict the power transfer efficiency according to the height. The results agree with the results of characteristic mode method using only 1 characteristic mode.

5.6 Summary

We investigated the effect of surroundings for WPT. To analyze the effect we introduce characteristic mode theory which is really helpful. First, The modified Z-matrix has been built as shown in (5.13). Then, the induced current on PEC plate is calculated using characteristic mode method. When PEC plate is small compared with antennas, the scattering field at the PEC plate is easily analyzed using only 1 characteristic mode. Our method is simple compared with other analysis techniques. Finally, the Theoretical results agreed with the simulation results

Reference

[1] Roger F. Harrington, Joseph R. Mautz, “Theory of Characteristic Modes for Conduction Bodies,” *IEEE Trans. Antennas and Propag.*, vol. 19, no. 5, pp. 622–628, Sep. 1971.

[2] R. F. Harrington and J. R. Mautz, “Computation of characteristic modes for conducting bodies,” *IEEE Trans. Antennas Propag.*, vol. AP-19, no. 5, pp. 629–639, Sep. 1971.

[3] D. Liu, R. J. Garbacz, and D. M. Pozar, “Antenna synthesis and optimization using generalized characteristic modes,” IEEE Trans. Antennas Propag., vol. 38, no. 6, pp. 862–868, Jun. 1990.

[4] A. El-Hajj, K. Y. Kabalan, and A. Rayes, “Characteristic mode formulation of multiple rectangular apertures in a conducting plane with a dielectric-filled cavity,” *IEEE Trans. Electromag. Compat.*, vol. 40, no. 2, pp. 89–93, May 1998.

[5] B. A. Austin and K. P. Murray, “The application of characteristic mode techniques to vehicle-mounted NVIS antennas,” *IEEE Trans. Antennas Propag.*, vol. 40, no. 1, pp. 7–21, Jan. 1998.

[6] R. F. Harrington, Field computation by Moment Methods, New York, MacMillan, 1968.

Chapter 6

Conclusion

In this thesis, various practical issues for implementation of WPTS was investigated. Proposed methods can be a help to implementation of WPTS.

In details, a modified frequency tracking method with a complex load matched at the target distance was proposed in chapter 2. Several adaptive matching methods used to achieve efficient WPT over a near-field region are compared. Although simultaneous conjugate matching demonstrates the best performance, it seems to be very difficult to implement. The performance of the frequency tracking method with a 50 ohm load is nearly the same as that of the simultaneous conjugate matching in the strongly coupled region. However, its transfer efficiency drops drastically as the distance between the two antennas increases beyond the strongly coupled region. Proposed method can achieve a stable efficiency beyond the strongly coupled region.

It was found that the effect of the dielectric loss of the plastic structure for fixing the antenna should be considered in the WPTS. In chapter 3, We suggested a new method used to achieve efficient WPT over a near-field region when the distance between the antennas varied. First, the conditions that achieve an efficient WPTS for the load resistance and mutual coupling between the antennas were suggested shown in (3.6). Then, we proposed the Class-D PA as a source of the WPTS. The Class-D PA has an advantage in regards to the efficiency of the source for a varied load resistance. To realize a WPTS when the coupling between two antennas is varied, our proposed system only needed to control the class-D PA and use a proper load resistance, and as a result, mutual coupling was satisfied (3.6). This method is simple when compared with the conditions of other methods when the operating frequency of the WPTS is fixed. In chapter 4, we propose a a time division technique for multiple receiver charging. By control of switches of receiver, we can make a condition of single receiver. We conclude that in terms of multiple receiver' charging, the proposed time division WPTS can transmit power efficiently and equally. In chapter 5, We investigated the effect of surroundings for WPT using characteristic mode theory. First, The modified Z-matrix has been built as shown in (5.13). Then, the induced current on PEC plate is calculated using characteristic mode method. It was found that the scattering field at the PEC plate is easily analyzed using only 1 characteristic mode when PEC plate is small compared with

antennas.

These proposed methods and analysis technique are useful to solve the adaptive matching and multiple charging problem and analyze the effect of surroundings for WPTS. I hope that this thesis helps to implement a WPTS.

Appendix

A.1 Computation of Generalized Eigenvalue Equation

We discuss solution of the matrix eigenvalue equation

$$[X][I] = \lambda [R][I] \tag{A.1}$$

The conventional method for reducing (A.1) to a symmetric unweighted eigenvalue equation requires [R] to be positive definite. In our problem [R] is positive semidefinite in theory, but because of numerical inaccuracies it is actually indefinite, with some small negative eigenvalues. We therefore modify the conventional method as follows.

Let [U] be the orthogonal matrix which diagonalizes R according to

$$[\mu]=\left[\widetilde{U}RU\right]=\begin{bmatrix}\mu_1 & 0 & 0 & \cdots\\ 0 & \mu_2 & 0 & \cdots\\ 0 & 0 & \mu_3 & \cdots\\ \cdots & \cdots & \cdots & \cdots\end{bmatrix} \qquad \text{(A.2)}$$

where the μ_i are the eigenvalues of R ordered $\mu_1 > \mu_2 > \cdots$. Premultiplying (A.1) by[U], and using (A.2), we obtain

$$\left[\widetilde{U}XU\right]\left[\widetilde{U}I\right]=\lambda[\mu]\left[\widetilde{U}I\right] \qquad \text{(A.3)}$$

Only the larger μ_i can be considered accurate, and we set all $\mu_i < M\mu_1$ equa1 to zero, where M is some small number set by our estimated accuracy of [R]. The diagonal matrix [μ] is then partitioned as

$$[\mu]=\begin{bmatrix}[\mu_{11}] & [0]\\ [0] & [0]\end{bmatrix} \qquad \text{(A.4)}$$

where $[\mu_{11}]$ contains all μ_i not considered zero. We also partition the other matrices in (A.3) conformably with $[\mu]$, i.e.,

$$[x] = \left[\widetilde{U} I\right] = \begin{bmatrix} [x_1] \\ [x_2] \end{bmatrix} \tag{A.5}$$

$$[A] = \left[\widetilde{U} X U\right] = \begin{bmatrix} [A_{11}] & [A_{12}] \\ [\widetilde{A}_{12}] & [A_{22}] \end{bmatrix} \tag{A.6}$$

Substituting (A.4) - (A.6) into (A.3), we obtain the two matrix equations

$$[A_{11}][x_1] + [A_{12}][x_2] = \lambda [\mu_{11}][x_1] \tag{A.7}$$

$$\left[\widetilde{A}_{12}\right]\left[x_1\right]+\left[A_{22}\right]\left[x_2\right]=0 \qquad \text{(A.8)}$$

The second of these may be solved for $[x_2]$, and the result substituted into the first to obtain the following matrix equation

$$\left[A_{11}-A_{12}A_{22}^{-1}\widetilde{A}_{12}\right]\left[x_1\right]=\lambda\left[\mu_{11}\right]\left[x_1\right] \qquad \text{(A.9)}$$

Now $[\mu_{11}]$ has only positive diagonal elements, and we can define the real matrix

$$\left[\mu_{11}^{1/2}\right]=\begin{bmatrix}\mu_1^{1/2} & 0 & 0 & \cdots\\ 0 & \mu_2^{1/2} & 0 & \cdots\\ 0 & 0 & \mu_3^{1/2} & \cdots\\ \cdots & \cdots & \cdots & \cdots\end{bmatrix} \qquad \text{(A.10)}$$

Substituting $[\mu_{11}]= [\mu_{11}^{1/2}] [\mu_{11}^{1/2}]$ into (A.9), and multiplying by $[\mu_{11}^{-1/2}]$, we obtain

$$\left[\mu_{11}^{-1/2}\right]\left[A_{11} - A_{12}A_{22}^{-1}\widetilde{A}_{12}\right]\left[\mu_{11}^{-1/2}\right]\left[\mu_{11}^{1/2}x_1\right] = \lambda\left[\mu_{11}^{1/2}x_1\right] \qquad \text{(A.11)}$$

This is now the real symmetric unweighted eigenvalue equation

$$[B][y] = \lambda[y] \qquad \text{(A.12)}$$

where the definition of [B] and [y] is obvious by comparing (A.12) with (A.11). The eigenvalues of (A.12) are the smaller eigenvalues of our original (A.1), and the eigenvectors of (A.12) give the corresponding eigenvectors of (A.1) according to

$$[I] = [Ux] = [U] \begin{bmatrix} [\delta] \\ [-A_{22}{}^{-1}\tilde{A}_{12}] \end{bmatrix} [\mu_{11}{}^{-1/2} y] \qquad \text{(A.13)}$$

where [δ] is the identity matrix.

초 록

본 논문에서는 무선전력전송시스템을 구현할 때 고려해야 하는 실질적인 문제들의 해결책들을 제시하였다. 고효율의 무선전력전송시스템을 구현하기 위해서는 아직 해결되지 않은 문제들이 많이 남아있다. 적응형 정합 및 다수의 충전 문제들을 해결하기 위해서 새로운 방법들을 제안하였다. 또한 특성모드 방식을 이용하여 주변환경이 무선전력전송시스템에 미치는 영향을 분석하였다.

우선, 근접장 영역에서 무선전력전송시스템을 위한 적응형 정합방법들이 연구되었다. 거리의 변화에 따른 근접장을 이용한 무선전력전송시스템의 임피던스와 공진주파수의 특성에 대하여 분석하였다. 근접장의 영역에서 고효율의 무선전력전송을 위해서는 적응형 정합방법이 필수적이다. 이 논문에서는 동시 공핵정합 및 주파수 추적방식을 포함한 다양한 방식의 전력전송효율을 비교하였다. 분열된 공진주파수를 추적하는 방법을 이용하면 효율적인 적응형 정합이 가능한 사실을 발견하였다. 또한, 고효율의 무선전력전송이 가능한 거리를 확장시키는 개선된 주파수 추적방식을 제안하였다. 이론적인 결과들을 실험결과와 비교하여 검증하였다.

두 번째로, 효율적인 무선전력전송시스템을 위한 최적의 조건을 제시하였다. 그리고 수신기의 위치에 따라 송신기의 입력저항이 변할 때 무선

전력전송시스템의 전력원으로 D급 전력증폭기를 사용하는 것이 유리하다. 실험을 통해서 이 논문에서 제안된 무선전력전송시스템을 증명하였다.

세 번째로, 무선전력전송시스템에서 다수의 수신기를 충전하는 방법을 제안하였다. 우선 근접장 영역에서 다수의 수신기가 가지는 주파수 특성을 분석하였다. 그 결과를 이용하여 시간분할방식의 무선전력전송시스템을 제안하였다. 제안한 방식을 이용하면 다수의 수신기에 고효율의 균등한 전력전송이 가능하다. 다수의 수신기를 충전할 경우 제안된 방식의 시스템의 유리하다는 결과를 확인하였다.

마지막으로 무선전력전송시스템의 주변환경에 대한 연구를 진행하였다. 주변환경의 영향을 분석하기 위해 특성모드 방식을 제안하였다. 전기적으로 작은 물체의 경우 그 물체의 전자기적인 반응은 소수의 특성모드만으로도 표현이 가능하다. 금속판과 작은 루프안테나의 시뮬레이션 결과와 제안된 이론을 통한 분석결과를 비교하여 검증하였다.

주요어: 근접장 결합, 무선전력전송, 적응형 정합, 주파수 추적, 공진 결합, D급 전력증폭기, 부하저항 조절, 다중충전, 시간공유, 특성모드

학번: 2008-30876